Shapes of Spacetimes – Collected tales of black holes

Emma Jakobsson

Shapes of Spacetimes

Collected tales of black holes

Emma Jakobsson

Cover picture by Linda Persson

ISBN print 978-91-7649-706-7
ISBN PDF 978-91-7649-707-4

Printed in Sweden by US-AB, Stockholm 2017
Distributor: Department of Physics, Stockholm University

Abstract

In theory, the existence of black holes is predicted by general relativity. In reality, there is a general consensus that they exist in space; in particular at the center of many galaxies. The theory of black holes has been around for decades, but there are still interesting questions calling for attention. This doctoral thesis and its four contributions touches upon some of these questions.

One challenging theoretical aspect of black holes lies in their definition, the event horizon. For several reasons, this definition is not satisfactory in many contexts, and alternative horizons based on the concept of trapped surfaces have been suggested to take its place. The question raised in Paper I has to do with the location of such surfaces in a simple model of gravitational collapse, the Oppenheimer-Snyder model.

A different scenario of gravitational collapse, that of a null shell of dust collapsing in flat spacetime, is the starting point of the original formulation of the Penrose inequality. By a reformulation, this inequality can be turned into a purely geometric relation in Minkowski space. In Paper IV we formulate and prove a $(2+1)$-dimensional version in anti-de Sitter space.

The Penrose inequality sometimes goes under the name of the "isoperimetric inequality for black holes". In Paper III a different kind of isoperimetric inequality is discussed (with less rigour), namely that of the volume contained in a black hole with a given area.

In Paper II, the subject of limits of spacetimes is visualized. Again, $(2+1)$-dimensional anti-de Sitter space finds its use, as a one parameter family of surfaces, capturing the geometry of charged black hole spacetimes, is embedded in it. Thus different limiting procedures are illustrated.

Finally, interesting models can be constructed by cutting and gluing in spacetimes, but in doing so one needs to take care, in order to obtain a physically realistic model. With this background as motivation, a study of Lorentzian cones is given.

Taken together, all of these contributions make up a collection of interesting aspects of black hole geometry, or, shapes of spacetimes.

Contents

List of accompanying papers

I **Trapped Surfaces in Oppenheimer-Snyder Black Holes**
I. Bengtsson, E. Jakobsson, and J. M. M. Senovilla
Phys. Rev. D **88** 064012 (2013).

II **Classics Illustrated: Limits of Spacetimes**
I. Bengtsson, S. Holst, and E. Jakobsson
Class. Quantum Grav. **31** 205008 (2014).

III **Black Holes: Their Large Interiors**
I. Bengtsson and E. Jakobsson
Mod. Phys. Lett. A **30** 1550103 (2015).

IV **A Toy Penrose Inequality and Its Proof**
I. Bengtsson and E. Jakobsson
Gen. Relativ. Gravit. **48** 156 (2016).

Paper not included in this thesis:

V **How Trapped Surfaces Jump in 2+1 Dimensions**
E. Jakobsson
Class. Quantum Grav. **30** 065022 (2013)

Author's contribution

Paper I — Under the guidance of I. Bengtsson I did all the calculations involving the weakly trapped surfaces described in Section IV, and I provided all the numerical results in the same section. I wrote Sections III-V. This paper was originally included in my licentiate thesis (Jakobsson, 2014).

Paper II — I did all the numerical computations rendering the stereograms and other computer generated images. This included figuring out how the results of Fig. 5 could be translated into Fig. 8 by the use of an isometry. I checked all the formulas appearing in the paper, and made comments on the text.

Paper III — All the calculations involved in the paper were done by me, and I provided the figures.

Paper IV — The results of the paper were obtained through an equal amount of effort from me and I. Bengtsson. I wrote the paper.

Preface

The writing of this thesis began on a November night. I had just read through the four papers accompanying it. These papers are quite different in character, both regarding their content, and in their approach to problem solving. And on this dark night I was thinking to myself: How can I tie these results together into a uniform thesis? Some of the questions asked are easy to formulate. For instance: How can we really know if we are inside a black hole or not? What is the volume of a black hole? Others are of a more theoretical character. But their answers all stem from understanding the geometry of spacetime. In particular, they all touch upon the geometry of *black hole* spacetimes, in one way or another.

Still, the subject of black holes is a broad one; more can be said about it than what is appropriate in the current format. So, instead of digging deep into one specific topic, this thesis provides a basic overview of the topics involved in the accompanying papers. The aim has been to make these topics accessible to a reader with a basic knowledge of relativity. A more knowledgeable reader might find the accompanying papers more stimulating, while the reader without any knowledge in general relativity will find even the overview difficult to follow. Still, the intention has been to give a descriptive and intuitive idea of these topics, and at best perhaps both of these categories of readers will find something to appreciate.

An outline of the thesis is given in the following. In Chapter 1 the most basic fact that gravity is geometry is stated, and we discuss how this geometry can be understood with the help of a splitting of spacetime into space and time, and by introducing Penrose diagrams. A compact picture of $(2+1)$-dimensional anti-de Sitter space, which is constantly recurring in the thesis, is also described. Chapter 2 reviews the most basic black hole spacetimes. The opportunity is also taken to, in this context, briefly discuss the topic of limits of spacetimes. The concept of black holes is then taken one step further in Chapter 3. We review the general definition and its implications, and introduce trapped surfaces and alternative black hole horizons. Chapter 4 is devoted to the topics of black hole volumes and the Penrose inequality. The thesis

ends with Chapter 5, where the technique of cutting and gluing in spacetime is discussed. In particular, properties of Lorentzian cones are investigated.

Acknowledgements

First of all I would like to express my gratitude towards my supervisor Ingemar. Thanks to his talent for finding interesting ideas, and his inspiring perspective on things, I have been able to enjoy my time as a Ph.D. student to the fullest. Even though both of us have very strong wills, our collaboration has been frictionless, and I have always gotten all the support and encouragement I needed.

My thanks go to Edvard and Fawad who have taken the time to read this thesis and helped me by suggesting improvements.

During these years I have learnt a great deal from numerous worthwhile discussions in the company of José Senovilla, whose friendly and encouraging attitude has been much appreciated.

I would like to acknowledge Jorma Louko and his contribution to this thesis by suggesting the ideas of Chapter 5.

The very small relativity group, which I have been a part of, would not be a group without the presence of Jan Åman. Also, the regular meetings on the initiative of Yen Chin Ong, have contributed to a creative environment.

To anyone who have given their support and made it possible for me to take on this journey, I am most grateful.

I thank all the present and former members of the condensed matter group for creating the friendly and relaxed working environment that is so important for all of us and the work that we do.

My office friends, Sören and Thomas, you have truly been a second family to me. The value of the safe environment you have provided can not be overestimated. You are the sunshines of my (office) life! Let us hope that this is not the end of an era.

Further contribution to the flourishing office environment has been given by the regular flow of visitors. In particular, I would like to thank Emma, Jonas, and Samuel for their company.

My old friends, Sarah, Ellen, Terese, Isa, Yaël, who have been with me from the beginning, even though you have not gotten the attention you deserve lately, know that you are important to me.

Thank you, mamma and pappa, for boosting my confidence with your immensely high thoughts of me, and for your endless support. And my beloved brother Oskar, where would I have been today if you hadn't taught me to walk and to read?

Selma, by sticking your cute little nose into my business, I have been reminded that sometimes it is more important to play with a toy mouse, than with a toy black hole.

Finally, thank you Jonas, my love. For your help in writing this thesis, by gently putting the laptop on my pillow, thus telling me to wake up from my feverish dreams and start working. And for being the perfect partner I once thought I would never find.

Detta är vad jag vet
stående här på ett ben i kärret:

Gunnar Ekelöf, Gymnosofisten

Chapter 1

Seeing spacetime

> Bedyrande vår oskuld sökte vi
> att utan formler popularisera
> och på det språk de flesta levde i
> en blygsam skymt av klarhet hopsummera
>
> *Harry Martinson, Aniara*

One obstacle I have often come across when trying to convey the theory of general relativity to others (and myself) is the difficulty of understanding a four-dimensional manifold. I often insist that the problem is not that of *understanding* but of *seeing* (and getting used to). One can easily get lost in a philosophical maze when contemplating space. By space I here mean the three-dimensional space that we are so familiar with in our everyday life. Most of us understand space through the objects living in it, through the separation in space between me and the sofa and the coffee-table with that tempting piece of chocolate on it. Ask the question "What is space without objects?" and you will most likely stare into a face shaped like a question mark. But the point is, that we "understand" space because we can *see* it, and because we are used to it. The aim of this chapter is to review techniques of visualizing spacetimes. In doing so, pictures that play a more or less important part in the accompanying papers are introduced. On top of that, the very definition of what a black hole is, is intimately related to some of these pictures, as will become clear in Chapter 3.

1.1 Slices

In the theory of general relativity, gravity is not due to a force, but to the curvature of spacetime. Imagine two hikers starting off at two different places

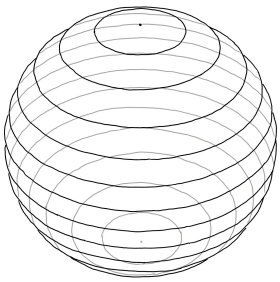

(a) A sphere cut into round circles.

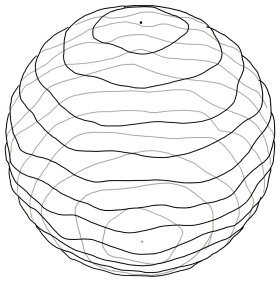

(b) An alternative slicing of the sphere.

Figure 1.1: Slicings of a sphere.

on the equator, beginning to walk straight north. Even though it would be difficult, these two hikers are steadfastly determined to keep this course during the entire walk. If they succeed in this, and if they persist long enough, their paths will finally meet at the north pole. They started out in parallel directions, but even so, if they keep the same pace, they will meet. Were they attracted to each other by a force? No, the "attraction" is due to the fact that they are confined to the surface of the Earth. The Earth is pretty much shaped like a sphere, and the sphere is a curved surface. That is why the two hikers' paths cross. And it is in this way that gravity works, but the stage is not the surface of the Earth, but *spacetime*. So in order to understand gravity we need to understand the geometry of spacetime.

The curvature of a surface—like the sphere—or a curve, is easy to visualize by an embedding in a larger dimensional space. But what if the hikers were two-dimensional creatures, that only have a sense for back and forth, and right and left, but not of up and down? The answer to how they could experience curvature lies in the way their "straight" paths behave relative to each other. But moreover, how could they even picture the sphere they are living on? One way of doing so is by slicing the sphere up into one-dimensional shapes. For example as a series of circles, shown in Fig. 1.1a. Our two-dimensional hikers can visualize these one-dimensional circles as shapes embedded in, for example, a plane. The whole sphere can then be understood as a sequence of circles of different sizes. If they begin to walk simultaneously, and keep the same pace, then at each instant of time they will find themselves on the same circle, and as they keep walking the circles become smaller with the result that the distance between them shrinks.

The simple example with the sphere is supposed to illustrate how we, as three-dimensional (or should we think of ourselves as four-dimensional?) beings can picture curved space as a sequence of curved surfaces, or spacetime

as a sequence of spaces. However, the sphere can be sliced up into curves of other shapes than round circles. For instance, the slicing shown in Fig. 1.1b. If the hikers choose to view the sphere in this slicing, it would most likely affect their intuition of the sphere and its curvature. In the same way we run the risk of being fooled by our intuition of spacetime, precisely because our intuition is based on a particular slicing. We tend to think of space and time as separate things, that is, in our heads we slice spacetime up in a series of constant time surfaces, a series of "nows", that is space. The fourth dimension, time, is then understood by letting each of these "nows" act as a frame in a film, one replacing the other as we push play. But it is important to keep in mind that in relativity there is no universal time—there is no absolute notion of "now"—meaning that the foliation we picture is not unique at all. It is therefore a good idea to be aware of whether one's understanding of a spacetime is based on a particular foliation, and, if so, test that understanding by playing around with other slices.

A stack of hyperbolic planes

There are questions in general relativity that are very difficult to answer. Often, one comes across a problem that just can not be answered by a simple calculation. But just as a lower dimensional space or spacetime is easier to visualize than a higher dimensional one, some of these questions are a lot easier to answer in lower dimensions. One way of effectively lowering the number of dimensions appearing in a problem is to make use of particular symmetries of the spacetime. Such a use of symmetries will be discussed a bit more in Section 1.2. A different approach is to simply look at a similar problem in a spacetime of lower dimension, in the hope that such a toy model can say something about the real problem. Both Papers IV and V (the latter not included in this thesis) deal with such toy models, and they both make use of the same spacetime: (2+1)-dimensional *anti-de Sitter space* (adS_3). This is a spacetime with two spacelike and one timelike dimension. It is maximally symmetric, it has negative curvature, and it is the perfect arena for black hole toy models. On top of that, it is easily visualized, and will therefore here serve as an example of what slicing and embedding can do for the eye. This example also provides a background to Papers II and IV, whose plots both take place on this stage.

Consider a flat spacetime with two spacelike dimensions and *two* timelike dimensions. Let us not dig too deep into the philosophical challenge of this exotic spacetime, as it will only serve as a tool to define the spacetime we are really interested in. If we choose coordinates (X,Y,U,V) such that the line element takes the form

$$\mathrm{d}s^2 = \mathrm{d}X^2 + \mathrm{d}Y^2 - \mathrm{d}U^2 - \mathrm{d}V^2 \,, \tag{1.1}$$

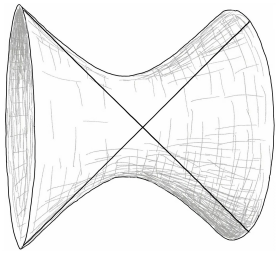

(a) A one-sheeted hyperboloid with two lightlike geodesics on it.

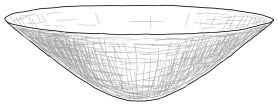

(b) A hyperbolic plane. All directions are spacelike.

Figure 1.2: Pictures of slices in anti-de Sitter space.

then adS_3 is defined as the hypersurface

$$X^2 + Y^2 - U^2 - V^2 = -\ell^2 \,, \tag{1.2}$$

embedded in this spacetime. The ℓ appearing in the definition above is just a constant setting a length scale, playing the same role as the radius when we define a sphere. The mathematics is simple and clear, but at this point a picture is impossible to draw. Let us therefore consider two different slices of this hypersurface. First we take a look at the slice of constant Y. This surface is a one-sheeted hyperboloid, depicted in Fig. 1.2a, embedded in a flat spacetime with two timelike and one spacelike dimension. The symmetry axis of the hyperboloid is a spacelike line in the embedding space, and closed curves going around the surface are actually timelike. This is in fact a picture of $(1+1)$-dimensional anti-de Sitter space, and it tells us that there is a lot of space, as we follow the hyperboloid to the left or right, far beyond the piece shown in the figure, and that time is periodic.

Next, let us define new coordinates t and T, as

$$\begin{aligned} U &= T\cos t \,, \\ V &= T\sin t \,, \end{aligned} \tag{1.3}$$

with $T \geq \ell$, and look at surfaces of constant t. The picture looks like the upper part of a two-sheeted hyperboloid—like the one shown in Fig. 1.2b—embedded in three-dimensional Minkowski space, with a timelike coordinate running along the symmetry axis of the hyperboloid. Surfaces of constant t are, in other words, two-dimensional hyperbolic planes. A picture of adS_3 has now emerged as a series of identical hyperbolic planes representing space at each "instant of time". The two pictures of Fig. 1.2 can also be understood together. We can view Fig. 1.2a as a picture of adS_3 with one spatial dimension

suppressed. Planes in the embedding space containing the symmetry axis of the hyperboloid will intersect the surface along hyperbolas. A picture of the full spacetime is obtained by letting each such hyperbola represent a hyperbolic plane. More work can be done to improve this picture of adS_3, but we leave that as a cliffhanger until the end of the next section.

1.2 Drawing infinity

We have seen how pieces of a spacetime can be visualized as surfaces embedded in a larger manifold. But the pictures, of for instance Fig. 1.2, still leave some work for the imagination, because the surfaces are simply too big to draw. They are cut off, because otherwise they would extend far beyond the pages of this book, all the way to infinity. But sometimes you just want your problem to fit on a piece of paper. This is one of the issues addressed in this section.

We have also discussed how a separation of space and time can be used to understand—in the sense of visualizing—spacetime. A warning was given though that such a separation can sometimes be misleading since space and time are fundamentally inseparable. One thing that is a bit obscured in such a picture is the causal character of spacetime. Sitting on my spacelike slice at an instant of time, and imagining a future slice, which regions of that future slice can I travel to? And which parts of a past slice can I see?

The superior method for catching the causal character of a spacetime on a piece of paper is the use of *Penrose diagrams* (Carter, 1966; Penrose, 1968). The result is most effective if the spacetime has some kind of symmetry. Often, we consider spherically symmetric spacetimes. Then the spacetime can be thought of as made up of homogeneous round spheres of varying sizes evolving in time. Restricted to a sphere, every point looks the same, obviating the need to distinguish between the different points. By simply letting a spacetime event be labelled by which sphere it sits on, and ignoring the exact location of the event on the sphere, we have, in a natural way, gotten rid of two dimensions and are left with only two dimensions, which goes perfectly well together with the number of dimensions available on a piece of paper. Next, we need to shrink down the size of the spacetime, which in most cases is spatially infinite, or extends infinitely to the future and/or past, or both. This shrinking is done by rescaling all distances by a conformal factor Ω, thus defining a line element

$$d\hat{s}^2 = \Omega^2 ds^2. \tag{1.4}$$

The factor Ω is chosen such that it tends to zero when distances given by the line element ds^2 diverges, so that all rescaled distances become finite. When

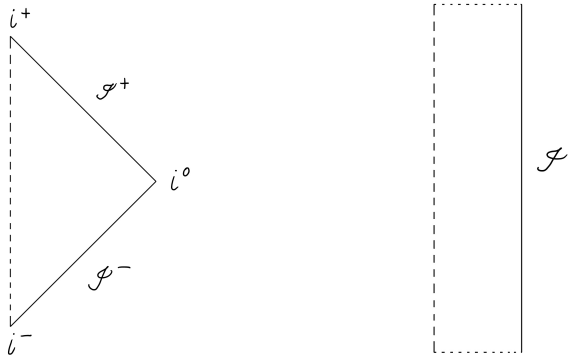

(a) Minkowski space. **(b)** Anti-de Sitter space.

Figure 1.3: Penrose diagrams.

the dimension is two, it is always possible to find a conformal factor such that the rescaled line element $\mathrm{d}\hat{s}^2$ is flat. Thus, this conformal map takes our two-dimensional spacetime into a finite region of (1+1)-dimensional Minkowski space. This shrinking is consequently called a *conformal compactification*. Thus, radial null geodesics are depicted as null geodesics most often are in Minkowski space, that is, as straight lines with a slope of 45°. The boundary of the finite region that the spacetime is mapped to—defined by $\Omega = 0$—is not a part of the spacetime, but is often added as an extra piece of structure. This boundary is called *conformal infinity* or $\mathscr{I}$ (pronounced "scri").

Let us make the idea a bit more precise by going through a couple of examples. A Penrose diagram of Minkowski space can be seen in Fig. 1.3a. As is customary in relativity, time flows upwards in the picture. Each point inside the triangle represents a sphere in Minkowski space, as was discussed above. The spheres grow in size as we move to the right in the picture, and the dashed line is the origin of our space coordinates, i.e. where the radius is zero. In the figure, the boundary is labelled by a few symbols; let us name these. The boundary consists of two parts: *past null infinity* $\mathscr{I}^-$ and *future null infinity* $\mathscr{I}^+$. They meet at *spatial infinity* i^0. The other ends are referred to as *past timelike infinity* i^- and *future timelike infinity* i^+, respectively. With this compact picture of Minkowski space, the fate of radial curves is now revealed. As already stated, the path of radial null geodesics will lie on a straight line with a slope of 45°. Thus we immediately see that they must all start on $\mathscr{I}^-$ and end up on $\mathscr{I}^+$. (As a geodesic meets the origin it will bounce off it in the picture as it proceeds, but this does not correspond to a real change of direction in the full spacetime.) A timelike geodesic always lies on a curve from i^- to i^+. But remember not to be fooled by the compactness of the diagram; this journey takes an infinite amount of proper time. A general timelike curve

also terminates at i^+, unless it is asymptotically lightlike, in which case it will end up at future null infinity. Finally, spacelike geodesics always terminate at spatial infinity, and, again, keep in mind that the metric distance along such a geodesic diverges as i^0 is approached.

The Penrose diagram of anti-de Sitter space in Fig. 1.3b looks quite different. Let us first translate it into the picture we already have of anti-de Sitter space. The hyperboloid of Fig. 1.2b being a spatial slice in adS_3 can be cut up into circles, just like we cut up the sphere in Fig. 1.1a. If we want to consider $(3+1)$-dimensional anti-de Sitter space instead, we can simply let each such circle represent a sphere; it does not affect the Penrose diagram. As before, every point in the Penrose diagram represents such a sphere. On the dashed line the radius is zero, and the further to the right the spheres are the larger they are, and as we approach $\mathscr{I}$ they become infinitely large.

While mentioning $\mathscr{I}$, we note that it is timelike in this case, and not lightlike as in Minkowski space. The causal nature of $\mathscr{I}$ is determined by the sign of the cosmological constant Λ (Penrose, 1968). Anti-de Sitter space solves Einstein's equations with a negative cosmological constant, in which case $\mathscr{I}$ is timelike, while $\mathscr{I}$ is lightlike for flat or asymptotically flat spacetimes. There is no future infinity in anti-de Sitter space. Recall that time is periodic, so we can think of the diagram as anti-de Sitter space cut open along the two horisontal dotted lines, which one may very well choose to identify if one wish. But the question of future infinity in anti-de Sitter space is a bit more subtle than that. It is common to extend the diagram of Fig. 1.3b into an infinitely long strip, by adding identical pieces to the future and past. This infinitely long strip represents the *covering space* of anti-de Sitter space, which is retrieved by performing identifications in the covering space. As it turns out, there is no future infinity even in the covering space. How this comes about is a complicated matter; it is discussed for instance by Di Carlo (2007).

And what about curves? Radial lightlike geodesics are depicted as they always are in Penrose diagrams. Spacelike curves start and end on $\mathscr{I}$. Timelike geodesics never reach $\mathscr{I}$, they just keep oscillating back and forth in the spacetime, while general timelike curves can reach $\mathscr{I}$.

With the diagrams of Fig. 1.3 we now have two spacetimes to put in our pockets. And more Penrose diagrams will appear in Chapter 2, where we will walk through a couple of black hole spacetimes.

A stack of disks

Now it is time to return to our stack of hyperbolic planes that was left dangling in the previous section. Since adS_3 is three-dimensional, one may wonder if we cannot draw a compact picture of the same dimension representing it. Then

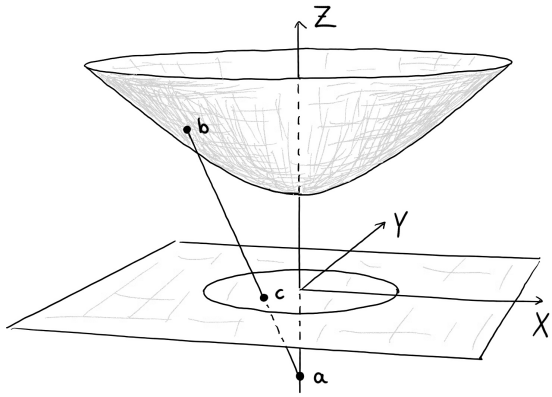

Figure 1.4: A projection of the hyperboloid into a plane.

we would actually be able to see the whole spacetime all at once, not having to imagine the extra dimensions that are suppressed in a Penrose diagram. This can be done, but light rays will no longer be depicted as straight lines, making it a bit more difficult to unravel the causal nature of curves and surfaces by just looking at the picture, compared to Penrose diagrams. The picture is still useful though, as Papers II and IV both demonstrate.

What has to be done in order to obtain the picture is simply to project each of the hyperboloids into a flat plane, in a way analogous to a stereographic projection of a sphere. The procedure can be seen in Fig. 1.4. First, we recall the definition of anti-de Sitter space given by Eq. (1.2). In this thesis the length scale ℓ seldom plays a major role and is therefore in most cases set to one. Let us adopt that standard from here on. Second, we refresh our memory on the coordinate change (1.3) and note that the hyperboloids at constant t are given by

$$X^2 + Y^2 - T^2 = -1\,, \qquad T \geq 1\,, \tag{1.5}$$

in Minkowski space where the metric is

$$\mathrm{d}s^2 = -\mathrm{d}T^2 + \mathrm{d}X^2 + \mathrm{d}Y^2\,. \tag{1.6}$$

Now we focus our attention on the point on the negative T-axis where T takes the value minus one. Let us call this point a, and choose a point b on the hyperboloid that we wish to project. The projection is now done by drawing a straight line between the points a and b, and project b to the point c where this line intersects the plane $T = 0$. If we do this for every point on the hyperboloid, the result is that it is projected onto the interior of a unit disk. This representation of the hyperbolic plane is called the *Poincaré disk*. No point on the hyperboloid is mapped to the boundary of the disk; this unit circle is our $\mathscr{I}$.

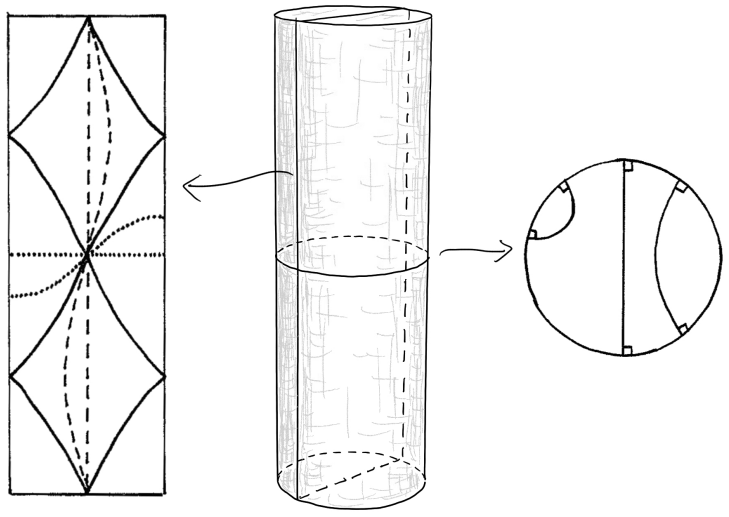

Figure 1.5: A picture of adS_3. Partly reproduced (Jakobsson, 2011).

The closer we are to the boundary, the more the metric distances on the disk are distorted. The distance from any point in the disk to the boundary is always infinite, no matter how close the point is to the boundary in the picture.

The full picture of adS_3 is now obtained by stacking these disks on top of each other forming a solid cylinder as in Fig. 1.5. The timelike coordinate t runs from 0 to 2π in the picture. The figure also shows some examples of geodesics on a couple of slices of the cylinder. On the vertical timelike slice lightlike geodesics are drawn as continuous curves, timelike geodesics are dashed, and the dotted curves are spacelike geodesics. On the Poincaré disk there is a simple recipe for finding geodesics; these are arcs of circles meeting the boundary at a right angle, or a diameter of the disk. More details on this picture of anti-de Sitter space are given in the Appendix of Paper II. An even more comprehensive description can be found in the standard reference on the subject (Holst, 2000).

Chapter 2

Black holes

> Ett enda steg på spårlös stig,
> och återvägen är mig stängd...
>
> *Karin Boye, En buddhistisk fantasi*

Up until now, we haven't even started mentioning the main theme of this thesis: black holes. The time has come to make amends for this. The popular description of a black hole is that of a region of space(time) where the gravity is so strong that nothing can escape from it. Since gravity is described by the curvature of spacetime, even light is affected as it follows its natural course on the curved background, and even light can not escape. That is why we call it a *black* hole, because we could never see what goes on inside, unless we were to venture into the hole ourselves.

A lot can be said about black holes, and a lot has been said about black holes; one simply has to pick up any textbook on general relativity, and they will be described in there. But in order to somewhat ease the accessibility of the accompanying papers to the reader not accustomed to these ideas, a review of the most basic black hole solutions will be given in this chapter. We start from the beginning with the Schwarzschild black hole.

2.1 Round and isolated

The theory of general relativity can be summarized with *Einstein's equation*:

$$G_{ab} = 8\pi T_{ab} \,. \tag{2.1}$$

The *Einstein tensor* on the left hand side reflects the geometry of spacetime, while the *stress-energy tensor* on the right hand side describes the matter content of the spacetime. The equation reflects how gravity is influenced by matter; two solutions with different matter content, also have different geometry.

As the geometry differs, so does the behaviour of the orbits of particles in it. But the left hand side also has its own dynamics even in the absence of matter. Thus we have to abandon the picture of spacetime as a fixed background on which we put our energy content; even the vacuum lives its own life.

Unfortunately, Einstein's equations are very difficult to solve. The first one to succeed was Schwarzschild (1916). He was particularly quick though; an often mentioned fact is that he came up with his solution only a few months after Einstein had published his vacuum equations (Einstein, 1915). The Schwarzschild solution is also the simplest non-trivial solution one can imagine (the trivial solution would be Minkowski space). In space, there are stars. These stars may not be perfect spheres, but nearly so. And the distances between them are often large. We have now given the physical arguments for considering the following situation: Imagine the empty space surrounding an isolated, massive, round object. What is the geometry of these surroundings? We turn to Einstein's equations and impose the following: we are in vacuum—i.e. the stress-energy tensor is zero—and the metric is spherically symmetric. To solve the equations we adopt the following coordinates: Space is made up of spheres and on the spheres we use angular coordinates θ and ϕ. The spheres have an area A, and we define an *area radius* r as

$$A = 4\pi r^2 \,. \tag{2.2}$$

Now, someone might object that A is simply the area of a sphere with radius r. Why did we take this detour, and not directly define r as the radius? We have to keep in mind that we are not in flat space, obviously, since we are looking for a non-trivial solution; distances may not be what we are used to. And how can we define a radius when the spheres have no center? We are considering the *exterior* of a massive object, so the solution we are looking for will have to be cut off where the matter region begins. So, it is safest to start with the area, which is a property of the sphere independent of the spacetime it lives in. There will also be a timelike coordinate which will be called t.

With this coordinate Ansatz, and assuming that the metric is independent of the angular coordinates, something remarkable happens when we solve the equations. It turns out that the metric of the solution can always be written on the form

$$\mathrm{d}s^2 = -V(r)\mathrm{d}t^2 + \frac{\mathrm{d}r^2}{V(r)} + r^2\mathrm{d}\Omega^2 \,, \tag{2.3}$$

where

$$\mathrm{d}\Omega^2 = \mathrm{d}\theta^2 + \sin^2\theta\mathrm{d}\phi^2 \tag{2.4}$$

is the metric on the two-sphere, and

$$V(r) = 1 - \frac{2M}{r} \,, \tag{2.5}$$

where M is a constant. This is the Schwarzschild metric in the standard coordinates. What is so remarkable about it is that it is the *unique* non-trivial, spherically symmetric vacuum solution (Jebsen, 1921). Also, the metric of this unique solution is independent of the timelike coordinate t. This means that there is a time-translational symmetry; spatial slices of constant t all look the same. The solution is *static*[1]. What more does the line element (2.3) tell us? We note that the larger r is, i.e. the larger the sphere we are sitting on, the closer the line element is to being flat. In other words, the further away we are from the gravitating object, the weaker its influence is. In the limit the metric becomes flat; the solution is *asymptotically flat*. The constant M determines the amount of curvature at a given r; in the Newtonian limit it corresponds exactly to the mass of the gravitating body. (Note that we use geometrized units, where masses, lengths and time intervals are all measured in the same unit by putting $c = G = 1$, where c is the speed of light, and G is the gravitational constant.) Further, we note that the line element (2.3) becomes singular when $r = 2M$. So, at a spatial slice of constant t our solution works perfectly well, until we reach this smallest sphere. For some reason, the surface of the star we imagine to give rise to the gravitational field, can not be smaller than this.

But this is not the full story. For decades it was unclear how to interpret the singularity at $r = 2M$. But the fact is that it is merely a flaw of the coordinates we are using. As a different choice of coordinates not exhibiting this feature was found—thus allowing an analytical extension beyond the boundary $r = 2M$—the secrets of the Schwarzschild metric began to unravel (Finkelstein, 1958). The *maximally* extended Schwarzschild solution was found by Kruskal (1960), and independently by Fronsdal (1959), who embedded it in a higher dimensional spacetime—a technique that, as we will see, also finds its use in Paper II. This maximal extension is best described by its Penrose diagram in Fig. 2.1. The diagram is divided into four blocks. Block I is the region that we have already discussed. It is bounded by past and future null infinity, and the lightlike hypersurface $r = 2M$. Passing the latter boundary to the future we reach region II. In fact, the standard coordinates that we used above are perfectly valid in this region too; it is only *at* $r = 2M$ that they break down. Thus, studying the line element (2.3), we see that the role of the coordinates t and r are interchanged, in the sense that t becomes spacelike and r timelike. As a consequence the spacetime is no longer static in this region. This also means that a journey into the future is equivalent to passing on to smaller and smaller spheres. It seems only natural that such a journey can not go on forever. Indeed, it ends at $r = 0$, represented by the wiggly line in the picture.

[1]This is true only if $r > 2M$; we will soon see why. In fact, the only globally static and asymptotically flat solution to Einstein's vacuum equations is Minkowski space (Einstein, 1941).

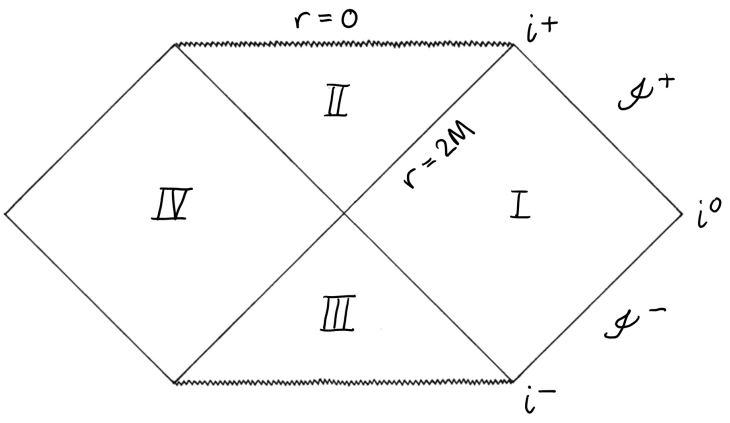

Figure 2.1: Penrose diagram of the Schwarzschild spacetime.

This is a true singularity where the curvature becomes infinite. Also by looking at the Penrose diagram we can readily draw the conclusion that there are no causal curves passing from region II to the exterior region I. As we will see in Chapter 3, the *black hole* is represented by block II, and the boundary between the black hole and its exterior is called the *event horizon*. Given this extension of the Schwarzschild solution it is perfectly possible for the surface of a round star to have an area radius smaller than $2M$. In that case both block I and II have to be taken into account when considering the exterior geometry, and the star has collapsed to form a black hole. More on gravitational collapse will come in Section 2.3.

While the two blocks that we have covered so far have a clear physical interpretation (at least as long as r is not too small), the two remaining blocks of Fig. 2.1 do not. Block III is identical to block II but time-reversed. It is bounded to the past by a singularity. Causal curves can, and do, leave this region, but do not enter it from any other region. The physical significance of this region can be debated, but it has been suggested, for instance, that it could be used to describe a bouncing scenario in which a collapsing body, due to quantum effects, eventually starts expanding again (Barceló, Carballo-Rubio & Garay 2014; Haggard & Rovelli, 2015). One of these models of a bouncing black hole will be discussed a bit more in Chapter 5.

Finally, block IV is an identical copy of block I, but the two regions are causally disconnected and can therefore never talk to each other. Most often, this region is considered unphysical.

2.2 Charge and spin

The Schwarzschild solution provides a natural introduction to black holes, but now it is time to move on. In this section we review two other important black hole solutions: The *Reissner-Nordström* spacetime describing a black hole with electric charge, and the *Kerr* spacetime describing a spinning black hole. Familiarity with the former is essential for comprehending Paper II, whose aim will also be summarized in this section. The Kerr black hole enters the stage in Paper III, but the idea of that paper will first be introduced in Chapter 4.

Reissner-Nordström

The Reissner-Nordström solution describes the exterior of a spherically symmetric object with both mass and *electric charge* (Reissner, 1916; Nordström, 1918). It is a solution of the *Einstein-Maxwell* equations, where the stress-energy tensor in Eq. (2.1) is not zero, but describes an electromagnetic field. The solution takes the same form as the Schwarzschild metric (2.3), but with

$$V(r) = 1 - \frac{2M}{r} + \frac{e^2}{r^2}\,, \qquad (2.6)$$

where the parameter e determines the strength of the electromagnetic field. If $e < M$ there are coordinate singularities at

$$r_\pm = M \pm \sqrt{M^2 - e^2}\,, \qquad (2.7)$$

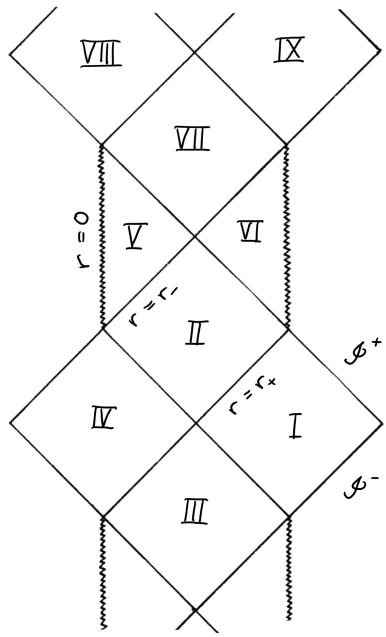

Figure 2.2: A Penrose diagram of the Reissner-Nordström solution.

and in that case the spacetime geometry is that of a black hole. The two hypersurfaces given by Eq. (2.7) are both different kinds of horizons. The outer horizon at $r = r_+$ is the event horizon of the black hole, and the inner horizon at $r = r_-$ is a *Cauchy horizon*. The existence of the latter has consequences for the predictability of the spacetime.

As in the Schwarzschild case, the Reissner-Nordström spacetime can be analytically extended beyond the horizons (Graves & Brill, 1960). A Penrose diagram of the full spacetime can be seen in Fig. 2.2. It is similar to the Penrose

diagram of the Schwarzschild spacetime in the sense that there are two causally disconnected asymptotic regions (blocks I and IV) which are asymptotically flat. The interior region II beyond the event horizon also has a time-reversed partner in region III. But instead of a singularity, block II is bounded to the future by the Cauchy horizon and the spacetime can be extended even further beyond that into blocks V and VI. Here we find *timelike* curvature singularities where the coordinate r is zero. The diagram can then continue into block VII which is an exact copy of block III. And from there continue on to two new asymptotic regions identical in structure to regions I and IV. The whole pattern can thus be extended infinitely to the future as well as to the past.

An observer falling freely into the black hole would not reach the singularity, but oscillate back and forth in the diagram, repeating its history forever. How much of this should be taken seriously, from a physical point of view? Theoretically, block I describes the exterior of a round object with electric charge—whether such objects are likely to exist in the universe or not is a different matter. If such an object would collapse and form a black hole, parts of block II would be needed to describe the exterior geometry. It is less clear what should be thought of blocks V and VI. In fact, starting with an initial value hypersurface reaching infinity in regions I and IV, it is impossible to predict the future of the Cauchy horizon. But due to instabilities of the Cauchy horizon, it is not unreasonable to expect that, in a physically realistic scenario, an effective singularity would develop in its vicinity (Simpson & Penrose, 1973; Poisson & Israel, 1990; Dafermos, 2005). This idea is tempting, since it would rid us not only of the seemingly unrealistic cyclic behaviour of the maximally extended Reissner-Nordström solution, but also of the issue of indeterminism caused by the existence of a Cauchy horizon. In general, it is conjectured that general relativity is a deterministic theory in generic situations; this conjecture is referred to as the *strong cosmic censorship hypothesis*.

There is also another aspect of singularities appearing in block II: A change of the value of the parameter e will not alter the appearance of the Penrose diagram. But lowering its value, and taking the limit all the way down to zero we retrieve the Schwarzschild solution. Then, in the limit, the diagram collapses. Singularities appear in blocks II and III, and the rest of the spacetime is cut off. A question one might ask is if it would be possible to pinpoint a hypersurface in the Reissner-Nordström solution where this happens. This question is addressed in Paper II, which deals with limits of the charged black hole.

The main theme of Paper II is a different limit though, namely the limit $e \to M$. Looking at the expression (2.7) for the two horizons, we see that they coincide when $e = M$. Thus, this limit also has a dramatic effect on the Penrose diagram, as can be seen in Fig. 2.3. The block between the two horizons has now suddenly disappeared, together with the second asymptotic region.

This spacetime is called the *extremal* Reissner-Nordström black hole. Although there is no evidence of such a black hole existing in nature, it has a number of interesting qualities. An example is that its surface gravity, and thereby its Hawking temperature, is zero. In other words, no Hawking radiation would be expected to be emitted by an extremal black hole.

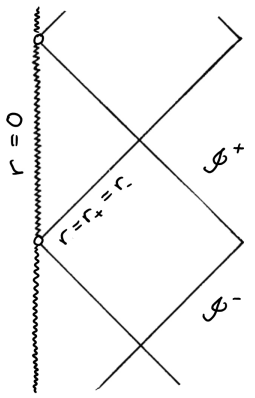

Figure 2.3: The extremal charged black hole.

Now, taking limits is not as straightforward as one might think at first sight; they are seemingly coordinate dependent! Accordingly, there exists at least one more limit $e \to M$ than the one discussed above. The real reason for why different limits come about was clarified by Geroch in 1969. He stated what choices one has to make in order to obtain a unique limit, thus providing an unambiguous definition of limits of spacetimes. The paper by Geroch is not very detailed when it comes to how to actually apply the definition, however. In Paper II we complement his definition by illustrating it in a novel way. Those two-dimensional surfaces that are explicit in a Penrose diagram, are embedded in (2+1)-dimensional anti-de Sitter space. Presenting the result in the compactified picture of adS_3, which was described in Section 1.2, we obtain a picture looking like a stretched and bent Penrose diagram. But the difference is that this picture will change as we vary the value of the parameter e, and in that way the "collapse" of the Penrose diagram in the limit, and what leads up to it, becomes visible.

Before we leave the company of the Reissner-Nordström black hole, a last remark is given. In the case $e > M$, the solution is not a black hole, but a spacetime with a *naked singularity*; that is, it contains a singularity not hidden behind an event horizon. The same would be true for the Schwarzschild solution, if the mass M were negative. But while negative mass seems unreasonable from a physical point of view, it is intuitively not very clear why the charged black hole must have an upper bound on its charge. A body, or a particle, that is not collapsing into a black hole, can exceed this bound without any problems. However, a widely believed assumption called the *weak cosmic censorship hypothesis* states that there can never be any naked singularities in nature (Penrose, 1969). We will later come back to this assumption, as it plays a role in the two following chapters.

Kerr

In Section 2.1 we looked for the simplest possible solution to Einstein's equations, and we found a black hole! They inevitably show up in theory, but do they exist? An astronomer would give a positive answer to that question. And not only are they likely to exist, but they spin as well (like so many other celestial bodies). The description of a spinning black hole was found by Kerr in 1963. This solution is not spherically symmetric, but axially symmetric. It is not static, but outside the event horizon it is *stationary*, meaning that there is a timelike Killing vector field, but one can not find spatial slices orthogonal to it. These two properties make it a lot more difficult to visualize the Kerr spacetime than the round and static solutions that we have reviewed so far. The lack of spherical symmetry makes it impossible for us to effectively illustrate its causal structure in a Penrose diagram. And the fact that it is not static prevents us from making a natural splitting of space and time which is so helpful for our understanding. Instead we will have to settle with less comprehensive pictures. These will not be presented here, however. Instead, the reader eager to learn more about the Kerr spacetime is referred to the book by O'Neill (1995).

2.3 More on collapse

The basic black hole spacetimes that have been reviewed in this chapter have all been vacuum, or—in the case of Reissner-Nordström—electrovac solutions of Einstein's equations. But the idea is that black holes are formed due to the collapse of *matter* (a star). In order to obtain a physically realistic description of a black hole collapse, we therefore need to bring some matter into the picture. In this section one of the simplest of such models is introduced; a model which is the subject of Paper I. It is called the *Oppenheimer-Snyder black hole* (Oppenheimer & Snyder, 1939). This model is obtained by cutting out pieces of two solutions to Einstein's equations, and gluing the pieces together. One of the solutions is the Schwarzschild spacetime, and the other is the *Friedmann universe* (Friedmann, 1922).

The Friedmann universe is a homogeneous and isotropic spacetime filled with dust. The spacetime geometry is described by the closed *Friedmann-Lemaître-Robertson-Walker* metric

$$\mathrm{d}s^2 = -\mathrm{d}t^2 + a^2(t)\left(\mathrm{d}\chi^2 + \sin^2\chi\,\mathrm{d}\Omega^2\right) . \tag{2.8}$$

A spatial slice at constant t is a three-sphere. The three-sphere—like the two-sphere—has no boundary; hence, space is *closed*. Its size is determined by the function $a(t)$, which is given explicitly by solving Einstein's equations with a given matter model. In the Friedmann universe, the matter consists of freely

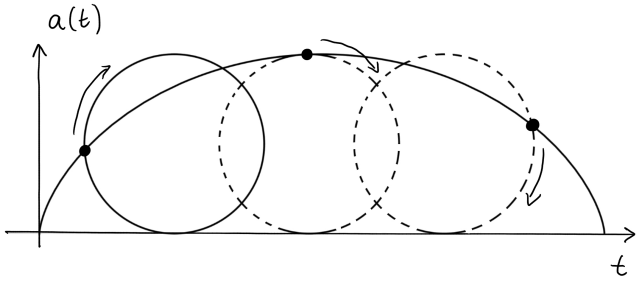

Figure 2.4: The cycloid.

falling dust particles. The term "dust" is used to indicate that these particles do not feel any pressure between them. Then, the solution for the function $a(t)$ is a *cycloid*. As can be seen in Fig. 2.4, its graph is obtained by the path a pebble stuck in a wheel would follow as the wheel is rolling along the t-axis. Thus, we see that this closed universe starts out from zero size—in a big bang singularity—then expands for a while, reaches a maximum size before it starts contracting again, and finally collapses in a big crunch.

The Penrose diagram of the Friedmann universe is not terribly complicated, as can be seen in Fig. 2.5. A horizontal slice at constant t is a three-sphere. Recall the slicing of a two-sphere into round circles that was discussed in Chapter 1, and depicted in Fig. 1.1a. In a perfect analogy, the three-sphere can be cut up into round two-spheres at constant χ. Each such two-sphere—as always represented by a point in the diagram—has an area radius $a(t)\sin\chi$. Moving from left to right on the horizontal slice, we thus start at the pole $\chi = 0$ where the radius is zero, move on to larger spheres until we reach a maximum, and then the spheres become smaller again until we reach the second pole. And the size of the largest sphere—the equator—is given by the value of a on the time slice in question.

We will now use a piece of the Friedmann universe to model the gravitational collapse of a cloud of dust. Consider a three-sphere at constant t. Now, we take less than half of this three-sphere, including two-spheres varying from zero size up to a maximum size at a chosen value of $\chi < \pi/2$. This largest sphere will be the surface of the dust cloud, and the rest of the three-sphere will be cut away, as we want to surround the cloud with vacuum. The surface of the cloud will thus be a time-like hypersurface at constant χ; a hypersurface fo-

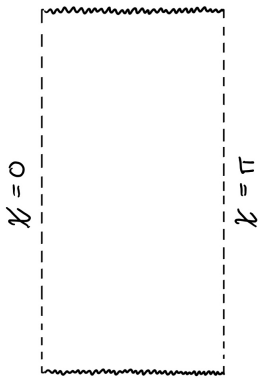

Figure 2.5: The Friedmann universe.

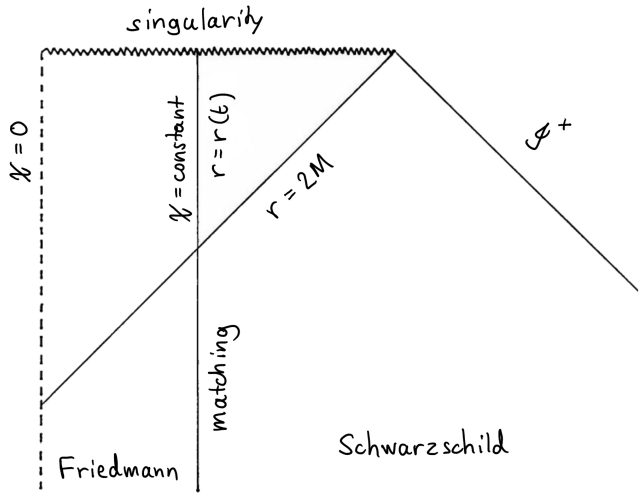

Figure 2.6: Penrose diagram of the Oppenheimer-Snyder black hole.

liated by round two-spheres varying in size with time t. Only the collapsing phase will be of interest. Then we match the cloud's surface to a fitting hypersurface in Schwarzschild, thus adding the exterior vacuum. This is the Oppenheimer-Snyder model, whose Penrose diagram can be seen in Fig. 2.6. The matching satisfies certain conditions, ensuring an appropriate amount of smoothness of the spacetime. We will say a few more words on this in Chapter 3, but the full details can be found in textbooks (e.g. Poisson, 2004).

In spite of its simplicity, the Oppenheimer-Snyder model is considered to give a reasonable account for what a gravitational collapse could look like. A broader picture is provided by the family of *Lemaître-Tolman-Bondi* solutions, of which the Oppenheimer-Snyder model is a special case. These all describe the collapse of spherically symmetric, but in general inhomogeneous, clouds of dust. As can be seen in Fig. 2.6 the weak cosmic censorship hypothesis holds in the Oppenheimer-Snyder solution. There is an event horizon given by the hypersurface $r = 2M$ in the Schwarzschild region, which is then extended into the matter region. But the same is not necessarily true in the general Lemaître-Tolman-Bondi solution (Christodoulou, 1984). However, these naked singularities could be an artifact of a matter model which, in itself, leads to infinite densities in a fixed Minkowski background. Indeed, for a better matter model, weak cosmic censorship has been shown to hold (Christodoulou, 1999).

In Paper I, the question under consideration is that of finding *trapped surfaces* in the Oppenheimer-Snyder black hole. The definition and meaning of such surfaces is the main subject of the next chapter.

Chapter 3

A boundary in spacetime

> Folk som inte har hav eller som har för lite hav vid sina länder får inte något begrepp om horisonten.
>
> *Gunnar Ekelöf, Verklighetsflykt*

In the previous chapter black holes were introduced through examples. But we have not said anything about how they are defined in general. In fact, the realization of a black hole is not as crystal clear as one might wish in many contexts. The exact solutions presented can not be expected to describe the whole complexity of nature; they are only simple models of certain aspects of our universe. But we believe that black holes exist, and therefore, we need to break free from the explicit solutions and generalize the whole concept.

3.1 The horizon

Let us analyze what happened in Chapter 2, starting from the beginning. We made a simple Ansatz in trying to find a solution to Einstein's equations and ended up with a black hole. Why? The solution we found contained a singularity, where spacetime suddenly ended. In fact all the non-trivial solutions we have reviewed share the same feature (except anti-de Sitter space). For some time it was suspected that this could be a consequence of the high degree of symmetry of these spacetimes, but in fact—and this is something we will come back to—singularities are a generic feature of solutions to Einstein's equations. The presence of a singularity is tightly linked to the presence of a black hole, but does not define it. For instance, the Friedmann universe contains singularities but this is not a black hole spacetime.

Before we move on, it is perhaps appropiate to make clear what is meant by a *singular* spacetime in general. When singularities appear in a solution,

it is not considered wise to regard them as a part of spacetime from a mathematical point of view. Instead, they are cut out. The definition of a singular spacetime can then not be that it contains singularities, since all singularities have been removed. Instead, a spacetime is said to be singular if it is *geodesically incomplete*. This means that there are geodesics in spacetime that end in finite parameter time.

In which cases, then, are singular spacetimes also black hole spacetimes? Let us try to identify what more our black holes have in common. In the examples we have studied, there have always been a notion of an interior region and an exterior region. The interior—the black hole—has been such that no causal curves can reach the exterior region. But what precisely is meant by the "exterior"? This is the question that needs to be asked; in order to define the black hole, we have to define its complement. The answer lies in the notion of conformal infinity.

Conformal infinity was introduced in Chapter 1 as a way of drawing compact little pictures of spacetimes. But its importance reaches a lot further than that, as already suggested. For instance, the very definition of a black hole relies on it. The Schwarzschild, Reissner-Nordström and Kerr black holes are all asymptotically flat. There is a notion of future null infinity and the blocks that have been referred to as the exterior regions are all contained in its *chronological past* $I^-(\mathscr{I}^+)$, while the interior regions are not. That is, from every event in the exterior a timelike curve may reach infinity. If the whole spacetime is contained in $I^-(\mathscr{I}^+)$—as Minkowski space is—then there is no black hole. But if it is not—and typically this can happen in the presence of a singularity—there is a black hole by definition. Accordingly, the event horizon is defined as the boundary of $I^-(\mathscr{I}^+)$, and beyond that boundary is the black hole. The definition captures an intuitive understanding of a black hole: Well inside not even light can "ever" "escape". The meaning of "ever" and "escape" are given by the notion of future infinity.

Even though a few details have been left out in this description, this is the basic idea behind the definition of a black hole. The major point is: without the concept of conformal infinity, no event horizon, and, it seems, no concept of a black hole. Thinking about it, this conclusion is rather unsatisfactory. Could it possibly be that we are passing the event horizon of a very large black hole at this precise moment of time? Well, that question could be given an answer only if we found out where the event horizon is. And in order to do that, we would have to gain knowledge about the infinite future of our universe.

The same problem is more relevant in numerical relativity. In order to explain it, a rough account of the intial value formulation of general relativity will be given. The existence of such a formulation is an essential part of the theory. An initial data set consists of a spacelike hypersurface with specified

initial conditions. These initial conditions consist of the spatial metric on the hypersurface, and the *extrinsic* curvature, describing how the hypersurface will be embedded in the spacetime that will be evolved from the initial data. In the next section, more details on the extrinsic curvature of surfaces will be given. But the intrinsic and extrinsic geometry can not be chosen arbitrarily if we seek for a solution to Einstein's equations. Four of these equations—they are ten in total—say nothing about the evolution of the hypersurface, but provide constraints on the initial data. Once an initial data set has thus been properly formulated, the rest of Einstein's equations in principle tell us how to evolve this space step by step in time yielding a spacetime solution. In practice, a lot of computer power is needed to perform this task. In that situation it would be practically impossible to tell if the initial data set is evolving into a black hole, unless there were some more local concept than the event horizon implying this. There is: the presence of a trapped surface.

3.2 The role of surfaces

Imagine a sphere. If you wish, you may deform it into the shape of a pear, or something even more interesting, as long as it remains a topological sphere. This surface is spacelike; it is only there at an instant of time. Now, imagine that at this very instant of time a flash of light is emitted orthogonally from every point on the sphere. In the intuitive picture that you have in your head—of a round sphere, a pear, or whatever it was you were thinking of—the flash of light can either be emitted outwards or inwards. Imagine that a flash of light is emitted in both directions. Then two wave fronts will form. If you have this picture in your head, my guess is that you see the ingoing wave front decrease in area, while the outgoing wave front increases. If so, abandon your picture and imagine instead that both wave fronts *decrease* in area. This is a trapped surface. Perhaps you find it difficult to imagine such a surface; it might be that you are stuck with a picture of space as something fixed. What you have to imagine is that space itself is shrinking so fast that not even the outgoing light rays can keep its pace. The presence of a trapped surface thus indicates a strong gravitational field. This will be discussed later in more detail, but let us first give some more rigour to the above somewhat loose description of a trapped surface.

Trapped surfaces

A trapped surface is always two-dimensional, closed, and spacelike. In principle this is not enough to claim that it is a topological sphere, but we will here only consider such. In order to make concrete some of the calculations appear-

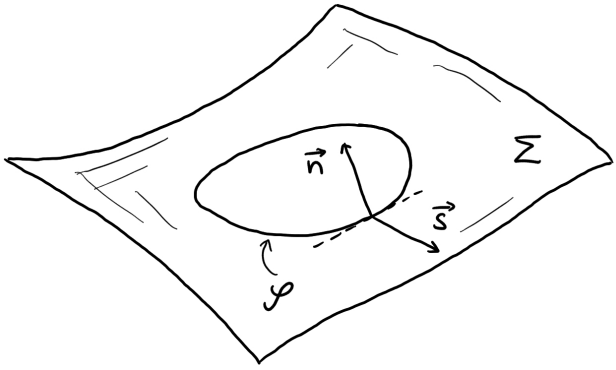

Figure 3.1: The surface $\mathscr{S}$ in a spacelike hypersurface Σ.

ing in this thesis, let us suppose that we have an explicit description of such a surface, and let us call that surface $\mathscr{S}$. Say that $\{x^\mu\}$, $\mu = 0,1,2,3$, is a set of coordinates on our spacetime, and that $\{y^A\}$, $A = 1,2$, is a set of coordinates on our surface, which is explicitly given by

$$x^\mu = x^\mu(y^A)\,. \tag{3.1}$$

At every point on the surface there is a set of two vectors $\{\vec{e}_A\}$ tangent to the surface, whose components in a coordinate basis are explicitly given as

$$e_A{}^\mu = \frac{\partial x^\mu}{\partial y^A}\,. \tag{3.2}$$

There are also two mutually orthogonal normal vectors to the surface at each point. For simplicity, let us assume that our surface lies in a given spacelike hypersurface Σ. Then we may readily identify two normal vectors to $\mathscr{S}$, which are illustrated in Fig. 3.1. For practical reasons one dimension is suppressed in the figure, so that Σ is drawn as a two-dimensional surface, and $\mathscr{S}$ as a one-dimensional curve. The figure still serves its purpose though: we see that the vector $\vec{n}$ is normal to Σ and therefore also normal to $\mathscr{S}$, while $\vec{s}$ is a normal to $\mathscr{S}$ that is tangent to Σ. We will assume that the hypersurface Σ is such that we can define an "outer" direction on it, and that the vector $\vec{s}$ is pointing in that direction, while the vector $\vec{n}$—which is necessarily timelike—is future directed. Both vectors will also be assumed to have unit length. Since the two vectors $\vec{n}$ and $\vec{s}$ are specified in terms of Σ, they are in no way special as normal vectors from the point of view of the surface $\mathscr{S}$. Any linear combination of $\vec{n}$ and $\vec{s}$ is also normal to the surface. In particular, they can be combined to form null vectors in two different directions:

$$\vec{k}^\pm = \vec{n} \pm \vec{s}\,. \tag{3.3}$$

For future reference, note that the normalization has been chosen as

$$\vec{k}^+ \cdot \vec{k}^- = -2 \,. \tag{3.4}$$

The vector $\vec{k}^+$ is called the *outer* null normal to $\mathscr{S}$, and $\vec{k}^-$ the *inner* null normal. These define the directions of the "flashes of light" that were sent out orthogonally from the surface in the introduction of this section. In some cases it might not be so straightforward to identify a spacelike hypersurface Σ containing the surface of interest. If so, one can still always find two null vectors orthogonal to $\mathscr{S}$, but the procedure described here often makes it a lot easier.

Let us move on to see how we can analyze the geometry of our surface $\mathscr{S}$. The induced metric γ_{AB} is given by the restriction of the spacetime metric $g_{\mu\nu}$ to the surface:

$$\gamma_{AB} = \vec{e}_A \cdot \vec{e}_B = e_A{}^\mu e_B{}^\nu g_{\mu\nu} \,. \tag{3.5}$$

This contains all the information about the intrinsic geometry of the surface. But for our purposes we need more; we need to know the surface's relation to its surroundings. So we shift our attention to how the surface is embedded in spacetime: its extrinsic properties. The starting point will be to consider a tangent vector field $\vec{e}_B$ on the surface, and figure out how it changes along the surface. The rate of change of the vector $\vec{e}_B$ at one point, in the direction of the vector $\vec{e}_A$, is given by the covariant derivative $\nabla_{\vec{e}_A}\vec{e}_B$ with respect to the spacetime metric $g_{\mu\nu}$. This resulting vector may be split up into two parts: one component tangential to and one component orthogonal to the surface. With a notation that will be explained gradually we may therefore write

$$\nabla_{\vec{e}_A}\vec{e}_B = \tilde{\Gamma}^C_{AB}\vec{e}_C - \frac{1}{2}\vec{K}_{AB} \,. \tag{3.6}$$

The first term is a linear combination of tangent vectors. The coefficients in front—we immediately see—are defined as

$$\tilde{\Gamma}_{CAB} = \vec{e}_C \cdot \nabla_{\vec{e}_A}\vec{e}_B \,. \tag{3.7}$$

These describe an intrinsic property of the surface: the connection, or, the covariant derivate on the surface. More interesting to us is the second term in Eq. (3.6). It is normal to the surface and can without loss of generality be split up into two components:

$$\vec{K}_{AB} = -K^-_{AB}\vec{k}^+ - K^+_{AB}\vec{k}^- \,. \tag{3.8}$$

The coefficients $K^\pm_{AB}$ have already implicitly been defined as

$$K^\pm_{AB} = -\vec{k}^\pm \cdot \nabla_{\vec{e}_A}\vec{e}_B \,. \tag{3.9}$$

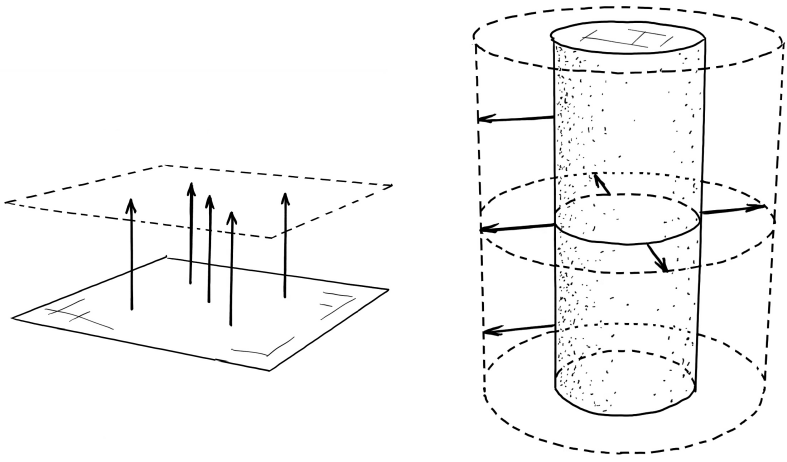

(a) A plane. **(b)** A cylinder.

Figure 3.2: Surfaces in Euclidean space and their normal vectors.

Alternatively, since $\vec{e}_B \cdot \vec{k}^{\pm} = 0$, we have

$$K^{\pm}_{AB} = \vec{e}_B \cdot \nabla_{\vec{e}_A} \vec{k}^{\pm} \,. \tag{3.10}$$

Thus we may also interpret $K^{\pm}_{AB}$ as describing the rate of change of the normal vectors $\vec{k}^{\pm}$ as we move along the surface. This interpretation intuitively captures the extrinsic curvature of the surface. Think, for example, of a flat plane in Euclidean space, whose normal vector is constant, and compare that to the surface of a cylinder in the same embedding space, where the normal vector keeps changing along the surface. See Fig. 3.2. Both the plane and the surface of the cylinder are intrinsically flat, but while the plane's extrinsic curvature is zero, the surface of the cylinder is curved in the embedding space.

The behaviour of light rays emanating from $\mathscr{S}$ can be described in terms of the extrinsic curvature of the surface. To see this, let us again consider the plane and the cylinder in Euclidean space. Straight lines emanating from the plane in the direction of its normal vector remain parallel. The same is true along a vertical line on the cylinder, since its extrinsic geometry is flat in that direction. But along a circular cut of the cylinder, the normal vector field is not constant; straight lines following the direction of outward pointing normals diverge as we move away from the surface. As a consequence the area of the whole cylinder will grow as we follow the flow of its normal vector field. This behaviour of geodesics emanating orthogonally from a surface in space or spacetime and its relation to the extrinsic curvature of the surface can be generalized. Returning to our surface $\mathscr{S}$ we define the outer/inner *null*

	θ^+	θ^-
Trapped	< 0	< 0
Marginally trapped	0	< 0
Outer trapped	< 0	anything
Marginally outer trapped	0	anything
Weakly trapped	≤ 0	≤ 0

Table 3.1: Definition of different classes of surfaces in terms of their null expansions.

expansion as the *trace* of the extrinsic curvature $K^{\pm}_{AB}$:

$$\theta^{\pm} = \gamma^{AB} K^{\pm}_{AB} \, . \tag{3.11}$$

If the outer null expansion θ^+ is positive at one point of the surface, then null geodesics in the direction of $\vec{k}^+$ around that point will tend to diverge. And replacing the word "positive" in the previous sentence with "negative", "diverge" will have to be replaced by "converge" in order to obtain a true statement. The definition of a trapped surface can now be stated as a surface $\mathscr{S}$ such that both its inner and outer null expansion are negative on the whole surface, in agreement with the illustrative description of a trapped surface given in the beginning of this section.

Let us end this basic review of the definition of trapped surfaces with a couple of remarks. There are many classes of surfaces related to the trapped surface described above. Some examples of these are given in Table 3.1. For a more extensive review of the terminology, the reader is referred to the zoological paper by Senovilla (2007). Note that these definitions are only concerned with the *signs* of the null expansions, and not their actual value. In fact, these exact values are not uniquely defined. Once we have found the null normals, they can be rescaled by a positive number σ, so that $\vec{k}^+ \to \sigma\vec{k}^+$ and $\vec{k}^- \to \vec{k}^-/\sigma$, while still keeping the normalization (3.4). This will affect the values of the null expansions, but not their signs. It may be well worth keeping this ambiguity in mind.

More horizons

The concept of trapped surfaces was introduced by Penrose in 1965. In the same paper their powerful use saw the daylight in the very first *singularity theorem*. Since then a number of singularity theorems have been formulated;

see for instance the review by Senovilla & Garfinkle (2015). These theorems say that under various physically reasonable assumptions, certain conditions inevitably lead to geodesic incompleteness. Thus the suspicion that singularities are a generic feature of solutions to Einstein's equations is substantially strengthened. A key player in many of these theorems is the trapped surface.

Without going into the details of the various singularity theorems, we can now give an outline of the general reasoning connecting trapped surfaces to black holes. Say that we find a trapped surface. Invoking the singularity theorems we then draw the conclusion that our spacetime is future geodesically incomplete, suggesting that a singularity will appear in the future. Now, if we believe in cosmic censorship—stating that this singularity can not be seen from future infinity—there must be an event horizon, and therefore, a black hole. Even though we have no clue about the evolution of our spacetime—we only know that in principle there is such an evolution, and we assume that there is a notion of future infinity—the presence of the trapped surface implies the presence of a black hole. And not only that: if there is an event horizon, then the trapped surface must lie inside it (Hawking & Ellis, 1973). This opens up the possibility of giving alternative definitions of black holes.

There is one context in which trapped surfaces already have the privilege of defining black holes: in the practice of numerical relativity. In a simulation where spacetime is represented by a set of spacelike hypersurfaces stemming from a finite evolution of an initial data set, the boundary of a black hole is defined by the *apparent horizon*. On each of the spatial slices the location of (marginally) outer trapped surfaces can be found with the help of effective algorithms (Thornburg, 2007). And the outermost marginally outer trapped surface on the slice defines the boundary, the apparent horizon.

The practical importance of trapped surfaces in numerical relativity immediately raises the question if they can be used to define black holes in more general contexts. Already, there is a handful of alternative black hole horizons available, which are based on the concept of trapped surfaces (see e.g. Ashtekar & Krishnan, 2004; Booth, 2005; Hayward 2013). Most of them are three-dimensional hypersurfaces foliated by marginally (outer) trapped surfaces, so called *marginally (outer) trapped tubes*. Such tubes go well together with some of the black hole boundaries already discussed. One is the apparent horizon of numerical relativity, which, as long as it satisfies certain stability conditions, is always contained as a leaf in a foliation of a marginally outer trapped tube (Andersson, Mars & Simon, 2008). The other is the event horizon of a stationary black hole. For example, every round sphere on the event horizons of the Schwarzschild and the Reissner-Nordström black holes are marginally trapped surfaces. But the growing part of the event horizon inside the dust cloud of the Oppenheimer-Snyder model is not. This will soon become clearer, as we

discuss the location of trapped surfaces in this model.

Another property that the stationary event horizons share is that they are *Killing horizons*; they are ruled by null geodesics generated by a lightlike Killing vector. Inspired by these facts we turn our attention to a special kind of marginally outer trapped tube: an *isolated horizon*. Such a lightlike three-surface is defined so as to include the relevant properties of a Killing horizon. It is thought to play the part of modeling an isolated black hole. There are a number of arguments for why this black hole must be isolated, one of them being that two-surfaces foliating the isolated horizon all have the same area. In contrast, a dynamical situation where the black hole is interacting with its surrounding is expected to display a growth of the horizon. Indeed, many numerical simulations give witness to apparent horizons making sudden jumps as they expand. When a black hole is evolving in this way, the notion of an isolated horizon is complemented by that of a *dynamical* horizon, which is a *spacelike* marginally trapped tube. A sudden jump of the apparent horizon is then explained by the fact that the marginally trapped tube it is necessarily a part of (as already mentioned), contains a spacelike portion. Unfortunately, an analytical description of such a dynamical situation is hard to come by, unless we lower the dimension of spacetime. This is done in Paper V. The starting point for the toy model there described is the BTZ black hole, which is a $(2+1)$-dimensional black hole obtained by cutting and gluing in adS_3 (Bañados, Teitelboim & Zanelli, 1992; Bañados, Henneaux, Teitelboim & Zanelli, 1993). By letting a lightlike particle fall into this black hole, it is seen how the isolated horizon makes a sudden jump outwards, as it grows in all directions. However, the marginally trapped tube in this model is discontinuous and does not contain a dynamical piece, but it does not seem unlikely that a refinement of the matter model could remedy this fact.

Before we leave the topic of marginally (outer) trapped tubes, a couple of remarks are worth giving. First of all, while a trapped surface, under the right circumstances, implies the existence of a black hole, there is no guarantee of the opposite: that a black hole implies the existence of a trapped surface. And even if a black hole spacetime is inhabited by trapped surfaces, they might not be visible in a given slicing. A striking example can be given in the Schwarzschild spacetime. The interior of the Schwarzschild black hole is filled with trapped surfaces; in particular, every round sphere at constant t and r is one. Even so, there are spatial slices not containing a single trapped surface, no matter how close the slices are to the singularity (Wald & Iyer, 1991). In the absence of an apparent horizon in this slicing, a numerical relativist could be led to believe that the Schwarzschild spacetime does not describe a black hole, even though we know that this is not the case. This also means that alternative black hole horizons in the form of marginally trapped tubes could be invisible

in certain slicings. However, they still provide an improvement compared to the event horizon, which is invisible in *every* slicing. Another disadvantage of marginally trapped tubes is rather the opposite: In general, it seems, there is an overwhelming abundance of them. On the one hand, this is probably a good thing in the context of numerical relativity, since a given time slice will most likely contain trapped surfaces, unless one is unlucky enough to choose a time slice as in the above example. On the other hand, this is a drawback if what one looks for is a uniquely defined boundary of a black hole.

In Paper I, a somewhat different approach to finding a candidate for the boundary of a black hole is investigated. That candidate is unique. It is likely that outer trapped surfaces can be found passing through every event in the interior of a black hole (this was conjectured by Eardley, 1998). Creative examples of how one can go about to find such surfaces are given by Ben-Dov (2007). But the same is not true for genuinely trapped surfaces. In general there will be a boundary between the region of spacetime where trapped surfaces occur and the region where they do not, which does not coincide with the event horizon in dynamical situations. We will simply call it the boundary. The idea is thus somewhat similar—but not perfectly analogous—to that of the apparent horizon in numerical relativity, but generalized to the whole spacetime. But while the numerical relativists have algorithms to find the outermost marginally outer trapped surface on a spatial slice, we are not even close to having the same tools in our search for the boundary.

Even in very simple cases it is remarkably difficult to find the boundary. In Paper I we investigate the matter in the Oppenheimer-Snyder model. Previous results show that in spherical symmetry there is a *past barrier*, a spacelike hypersurface to the past of which no trapped surfaces can enter (Bengtsson & Senovilla, 2011). The past barrier lies inside the event horizon, thus showing that the event horizon can not be a marginally trapped tube in the Oppenheimer-Snyder model. The results of Paper I narrows down the possible location of the boundary even further in the model in question. The strategy is to explicitly construct weakly trapped surfaces, designed so as to pass through the center of the dust cloud at earliest possible time. Even though we believe that the result of Paper I is close to being optimal, it has not been proven. But at least, we have definitely found a future temporal bound on the location of the boundary, complementing the role of the past barrier.

The task of constructing the surfaces involves some technical details due to the matching of the dust cloud with the Schwarzschild exterior. In the Oppenheimer-Snyder model, two timelike three-surfaces—one in the Friedmann universe, and one in the Schwarzschild spacetime—are glued together. These are chosen so that they have the same intrinsic and extrinsic curvatures, and we require that our surfaces are continuous in the same regard. This

complication was glossed over in an earlier paper on trapped surfaces in the Vaidya model (Bengtsson & Senovilla, 2009). The Vaidya spacetime is—like the Oppenheimer-Snyder model—obtained by gluing together spacetime solutions (Vaidya, 1951, 1953). But instead of a collapsing cloud of massive dust, it describes a spherically symmetric collapse of null matter. Such collapses play an important role in the next chapter.

Chapter 4

The isoperimetric problem

Grymta månde grisarna, om de visste vad den gamle galten lider.

Ragnar Lodbroks saga

Say you have a piece of string, and you want to arrange that piece of string on your desk so that it encloses the maximal possible area. How would you do that?

This is the *isoperimetric problem*. Sometimes it is also referred to as "Dido's problem". According to the legend, Dido founded the city-state of Carthage, by asking for a small piece of land, not more than what could be encompassed by an oxhide. Clever as she was, she cut the oxhide into thin strips, and thus managed to enclose a piece of land large enough to fit a whole city. The same story also appears in an old norse saga about the viking Ragnar Lodbrok and his sons. In avenging his father's death, the oldest son Ivar the Boneless uses the same trick for taking control over the city of York.

So, what is the answer to the problem? In order to enclose the largest possible area, the string of oxhide should be arranged into the shape of a round circle. Once this answer has been given away, we can conclude that the area A of any plane figure is related to the length L of its perimeter by

$$4\pi A \leq L^2 \,. \tag{4.1}$$

This isoperimetric inequality can be generalized to geometrical shapes in higher dimensional Euclidean spaces, relating for instance the volume contained in a closed surface to the area of that surface.

In this chapter, a background to Papers III and IV will be given. Both of them are related to the isoperimetric problem, but in a spacetime context, as we will see.

4.1 Black hole volumes

Consider the following question: Given a closed spacelike two-surface, what is the spatial volume contained in it? If you paid attention in Chapter 1, then you understand that this is not a well defined question. We have to make clear what is meant by "space", and as already discussed, there is a lot of freedom in separating spacetime into space and time. The volume we ask for depends on how we choose the three-dimensional spatial slice containing the surface. Only once we have picked out a specific slice, can we give a definite answer to our question.

By slightly altering the question we can obtain something similar to the isoperimetric problem: Given a closed spacelike two-surface, what is the *maximal* spatial volume contained in it? In Minkowski space, the answer to this question actually *defines* the spatial volume. But in curved spacetimes, the answer one finds can be remarkably unintuitive. In a paper by Christodoulou and Rovelli (2015) this problem is considered in the context of spherically symmetric gravitational collapse. Taking a cut of the event horizon with area radius $2M$, they find that the maximal volume it encloses grows with time; the longer we wait after the collapse of the matter, the larger the volume of the black hole becomes. In principle there is no upper bound on how large this volume can be. They find that the black hole at the center of our galaxy, which has an area radius of order 10^6 km—it would fit well inside the orbit of Mercury—and age $\sim 10^9$ years, would contain a volume large enough to fit a million solar systems!

But the black hole at the center of our galaxy spins, and this raises the question whether the result would be similar in a Kerr spacetime. This is the problem considered in Paper III, and the answer is yes. Even though the "isoperimetric problem" is not solved, we show that a specific choice of spatial slice gives a result of roughly the same order of magnitude as in Christodoulou's and Rovelli's paper. Accompanying that result, is a discussion on the trustworthiness of the result; it is argued that the large volume persists, even if large parts of the interior of the black hole were to deviate from the model used in deriving the volume.

Indeed, it does seem like black holes hide large volumes of space. Since Paper III was published, it has been shown by Ong (2015) and Christodoulou & De Lorenzo (2016) that even if a black hole emits Hawking radiation—and its area decreases—its volume still grows with time!

4.2 The Penrose inequality

The subject of this section is the famous Penrose inequality—sometimes also referred to as the isoperimetric inequality for black holes (Gibbons, 1984). First, we will give a review of the origin of the inequality (Penrose, 1973), and then give a summary of the work of Paper IV.

If one finds the thought of naked singularities exciting, then one might wonder if it would be possible to in any way cast doubts on the cosmic censorship hypothesis. This is what Penrose attempted when he formulated his inequality. The scenario he envisaged and the arguments leading up to the result will be given in the following. Consider an infinitesimally thin, collapsing null shell of dust, represented by the black cone-like surface in Fig. 4.1. Again, a three-dimensional hypersurface is drawn as a two-surface. If you find it difficult to read the picture, then slice it up in a sequence of horizontal planes representing space at an instant of time (this is actually true only for the lower part of the figure, so let us stick to that). On such a slice you find a closed two-surface where the null shell is. And as time goes on—upwards—the shell contracts with the speed of light as it collapses. This collapse takes place in Minkowski space; or, more precisely, before the shell has made its entrance spacetime is flat, but after the shell has passed it is curved. The exact exterior geometry depends on the shape and energy content of the shell, but we will have no need for its detailed properties. The only assumption we

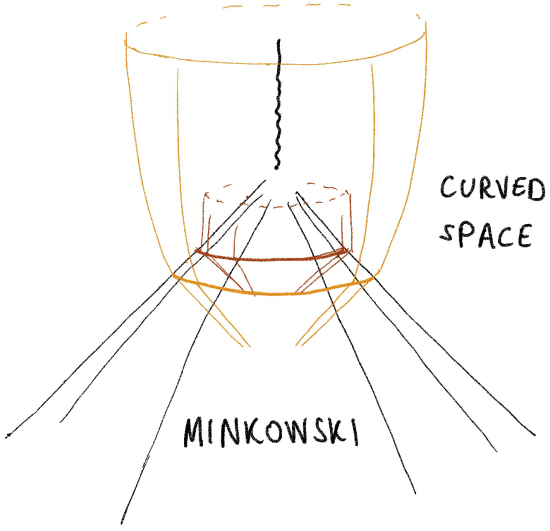

Figure 4.1: A collapsing null shell of dust in Minkowski space. The figure is a replica of Penrose's original (1973).

make is that the exterior is vacuum; no more radiation is falling in after the shell has passed. Now, consider the orange expanding null hypersurface starting out in the Minkowski region. As it passes the collapsing shell it will tend to be focussed. This is quite intuitive, given the attractive nature of gravity; mathematically it follows from Raychaudhuri's equation. The exact amount of focussing depends on the energy density of the shell, and as the shell contracts even more, becoming denser, it seems likely that an expanding null hypersurface in the Minkowski region could cease to expand altogether due to the shell. This is depicted by the brownish red hypersurface in the figure. In that case, the intersection of this hypersurface with the shell is a marginally trapped surface. This scenario can, in fact, always be designed. By adjusting the energy density of the shell, any spacelike cross section of it can be made into a marginally trapped surface. With the presence of a marginally trapped surface then comes the whole sequence of arguments already discussed in Chapter 3: A future singularity (wiggly black line), an event horizon (if we believe in cosmic censorship), a black hole. On top of that, the marginally trapped surface can not extend outside of the event horizon. Thus, the event horizon—wherever it is—must intersect the collapsing shell before the marginally trapped surface appears, unless it coincides with it. If A is the area of the marginally trapped surface, and A_{EH} is the area of the event horizon on the shell, we thus draw the conclusion that

$$A \leq A_{EH} \, . \tag{4.2}$$

The above relation can now be continued into a whole string of inequalities. As this black hole keeps evolving, the area of the event horizon can not shrink; it must either grow or stay the same. This is due to the area law for black holes (Hawking & Ellis, 1973). We expect the black hole to eventually settle down to a Kerr solution, and the area A_{EH} must therefore be less than or equal to the area of the Kerr event horizon. And the event horizon of the spinning black hole is greater the less it spins. If the mass of the final black hole is M_{BH}, then the area of its event horizon must consequently be less than or equal to $16\pi M_{BH}^2$, which is the area of the Schwarzschild event horizon. Finally, since no further mass or radiation is falling in, this mass can not be greater than the total mass M of the collapsing null dust. It could be smaller though, in the event that gravitational radiation is being emitted. To sum up the whole line of arguments, we conclude that

$$A \leq 16\pi M^2 \, . \tag{4.3}$$

This is the Penrose inequality.

It is saturated when the whole scenario is spherically symmetric. In this case the collapsing null dust must have the shape of a past light cone of a point,

and we know that the exterior spacetime must be Schwarzschild, because of the uniqueness of this solution. Furthermore, due to the spherical symmetry, a marginally trapped surface on the shell must be a round cut. And marginally trapped round surfaces in the Schwarzschild spacetime can only be found on the event horizon. So this round cut of the shell must coincide with the event horizon, and thus its area is given in terms of the Schwarzschild mass. Finally, this mass must be equal to the total mass of the collapsing null dust, since the spherically symmetric vacuum solution is static, taking away the possibility of emission of gravitational waves.

Let us recall the original motive for formulating the inequality. If we could find a counterexample to this inequality, then one or more of the assumptions used in deriving it must be false. Could it be the uniqueness of the Kerr solution? Or the cosmic censorship hypothesis? It does not really matter. Penrose failed in trying to do this, and the focus quickly shifted to trying to prove it. So far, it has been proven to hold true in many cases (Gibbons, 1973; Tod, 1985; Bergqvist, 1997; Sauter, 2008; Mars & Soria, 2012, 2014, 2016; Brendle & Wang, 2014; Roesch, 2016), but no full proof of the inequality, as it has been presented here, has yet been put forward.

Since it was formulated, the Penrose inequality has broken free from the original setup described here. In general, it is believed to hold for the area A of a suitably defined marginally trapped surface on an asymptotically flat spatial hypersurface with ADM mass M. In this formulation, the Penrose inequality provides a strengthening of the positive mass theorem which was proven by Schoen & Yau (1979, 1981) and Witten (1981). At the very same conference where Penrose presented his inequality, Geroch (1973) proposed a strategy for proving the (at the time unproven) positive mass theorem. Little did they know that Geroch's approach would later be taken up by Jang & Wald (1977) in an attempt to prove the *Riemannian* Penrose inequality. This inequality is the special case one obtains when the spatial hypersurface has vanishing extrinsic curvature. Many years later the Riemannian Penrose inequality was proven in full generality (Huisken & Ilmanen, 2001; Bray, 2001).

Let us return to what will be referred to as the null version of the inequality, where marginally trapped surfaces on null shells are considered, and reformulate it. Recall the reasoning that made it seem plausible that a trapped surface appears on the collapsing null shell: that the energy density of the shell determines the amount of focussing of the initially expanding null hypersurfaces. In fact, the discontinuous jump of the expansion across the shell is proportional to the mass density of the shell. If the cross section $\mathscr{S}$ is marginally trapped, this jump must be precisely equal to the outer null expansion θ^+ evaluated on the *Minkowski* side of the shell, in order for the expansion to be zero on the other side. The mass M of the shell can be obtained by integrating the mass

density over the marginally trapped surface $\mathscr{S}$, or equivalently, by integrating θ^+ over the surface. Thus the inequality (4.3) can be rewritten as[1]:

$$\oint_{\mathscr{S}} \theta^+ \, \mathrm{d}S \geq \sqrt{16\pi A} \, . \tag{4.4}$$

And this is quite remarkable: The inequality (4.4) contains properties of the surface on the Minkowski side of the shell *only*. Hence it is a purely geometric inequality, quite like the original isoperimetric inequality in Euclidean space.

If the appearance of the alternative formulation (4.4) of the null Penrose inequality seemed quick, a more detailed sketch of its derivation is described in Paper IV. As can be seen there, the presence of a timelike Killing vector field is important, both for fixing the normalization of the null normals, and in defining the mass of the null shell. In Paper IV a *toy version* of the null Penrose inequality is formulated and proven. The form of this inequality is guessed by simply mimicking the above derivation of the original version. The full details of the physical interpretation are not investigated in the paper, but instead the emphasis is put on the geometrical aspect of the problem. As such, it gives a relation between the length L and the outer null expansion θ^+ of certain curves γ in adS_3:

$$\frac{1}{2\pi} \oint_{\gamma} \theta^+ \, \mathrm{d}l \geq 1 + \left(\frac{L}{2\pi\ell} \right)^2 \, . \tag{4.5}$$

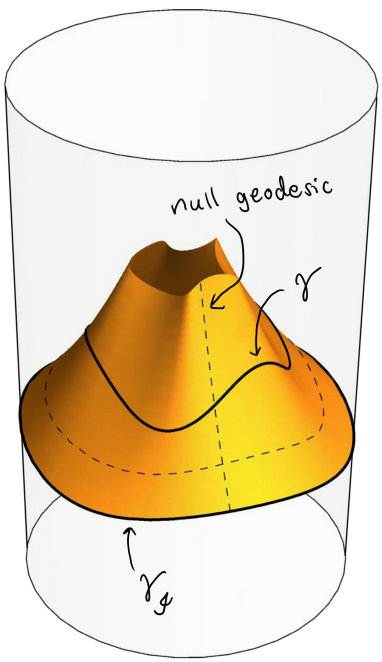

Figure 4.2: A null surface in anti-de Sitter space.

The approach to proving this relation is depicted in Fig. 4.2. The starting point is a null surface in anti-de Sitter space, representing a collapsing null shell. This surface is ruled by null geodesics, one of which is drawn as a dashed curve in the figure. Eventually, the null geodesics will inevitably begin to intersect and caustics will appear, which is exactly what happens where a sharp peak can be discerned

[1]Here an extra condition has been put on the normalization of the outer null normal vector in order to fix the value of the outer null expansion; recall the discussion on p. 27.

on the future end of the surface in the picture. However, recall that in the original formulation we were considering a collapse in flat spacetime, which can only be guaranteed if the null shell is free of caustics to the past. Here, we will stick to the same requirement, and the strategy for ensuring that this condition holds, is to define the null surface in terms of its past intersection with $\mathscr{I}$. This is the smooth curve $\gamma_{\mathscr{I}}$. The class of spacelike curves γ for which the inequality (4.5) is to be proven, must then lie on the null surface, but below the point where caustics first appear. In this way, the problem involves two free functions: one of them describes the shape of the null surface through the curve $\gamma_{\mathscr{I}}$, and the other describes the shape of the curve γ on the surface. The length and outer null expansion of γ can be expressed in terms of these two functions, showing the validity of the inequality (4.5).

Apart from being interesting in its own right as a new geometrical inequality for curves in anti-de Sitter space, one may wonder how the inequality plays its part as a toy version of the original Penrose inequality. The strategy used in proving it is quite different from the most common approach to the original problem in Minkowski space. Instead of letting the curve be the starting point, and trying to figure out under which conditions the inequality is supposed to apply to it, we begin by describing a general null shell with the required properties. It would be interesting to see if the same approach could prove successful in other variations of the problem. In conversations with Ingemar Bengtsson and Thomas Bäckdahl, strategies for tackling an analogous problem in $(3+1)$-dimensional anti-de Sitter space have been discussed. It remains to see whether these ideas will prove fruitful or not.

Chapter 5

Lorentzian cones

This chapter is devoted to the subject of cutting and gluing, and the nature of conical singularities arising from such procedures. Let us introduce the subject by presenting a simple exercise that can be practiced at home with a piece of paper, a pair of scissors, and a ball of suitable size. Cut out a wedge of the piece of paper and glue the edges together, as in Fig. 5.1. Thus a cone has been created. This cone has a sharp tip, and one can think of reasons for not being happy with this feature. If that is the case, take a look at Fig. 5.2 for a solution to the problem: Cut away the tip of the cone (red) along a round circle, and take a piece of a sphere (green) to replace the tip with. Now, any sphere will not do; it must have the right size. The circle along which the sphere is cut must have the same length as the circle bounding the tip of the cone, or otherwise the pieces will not fit together. Furthermore, if we want the resulting surface to feel smooth when sliding a finger across it, an extra condition is needed. The requirement needed is that the two circles have the same geodetic curvature; that they deviate by the same amount from being geodesics on their respective surface. These two conditions are in fact the

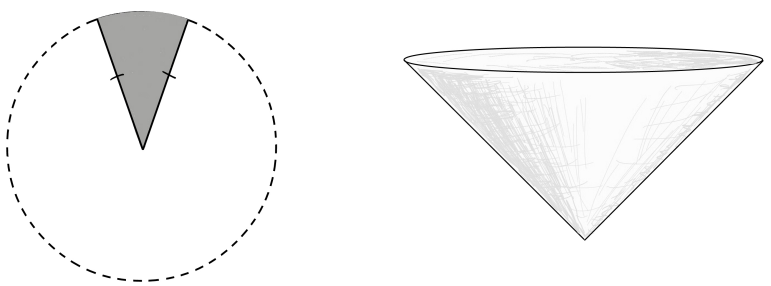

(a) Cut out a wedge... **(b)** ... and glue the ends together.

Figure 5.1: A cone.

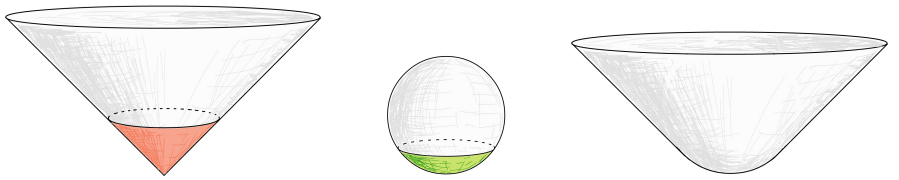

Figure 5.2: Making a cone smooth.

same as those discussed in the context of the Oppenheimer-Snyder model in Chapter 3, where two three-surfaces were required to have the same intrinsic and extrinsic geometry.

The question we now ask is: Can something similar be done in *spacetime*? Before the answer is investigated, the context in which the question was first proposed will be given.

Motivation

Haggard and Rovelli (2015) created a model in which null matter collapses into a black hole, but then—due to unknown quantum effects—bounces, and comes out again from a white hole. The model is depicted in Fig. 5.3b. The shaded region is a piece of the Schwarzschild spacetime, chosen as in Fig. 5.3a. This partly overlapping region is opened up and connected to a quantum region—labelled by a question mark in the figure—, while the past and future ends are glued onto pieces of Minkowski space along to lightlike hypersurfaces representing the bouncing null matter. The spacelike hypersurfaces of Schwarzschild connecting to the quantum region are not specified in detail, but as they are described, they can in fact not be chosen to be ruled by spacelike radial geodesics. This is because the point $\mathcal{E}$ in the figure lies in the "shadow zone" of Δ, as defined by Fuller and Wheeler (1962).

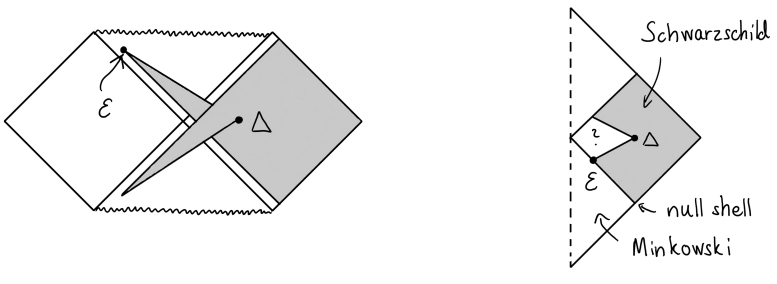

(a) **(b)**

Figure 5.3: Modeling a bouncing black hole.

A number of questions regarding this construction were raised in a discussion with Jorma Louko. Is it harmless to do this kind of violence to the Schwarzschild spacetime, or may there be unwanted consequences? Say that we were to ignore the quantum region, and instead directly identify the two spacelike hypersurfaces bounding it. Then a conical singularity would be present, located at Δ in Fig. 5.3a. What is the nature of this conical singularity created? Can the spacetime be made smooth[1] in a manner similar to the above procedure with the Euclidean cone? With these questions we have found the motivation to study Lorentzian cones. We will consider the simplest examples of such cones, namely cones in $(1+1)$-dimensional Minkowski space.

But before we do that, let us illustrate what could go wrong in a construction like Haggard's and Rovelli's. Apart from being a spacetime problem, it differs from that of the ordinary cone in one more regard. While the ordinary cone was produced by cutting *away* a piece of space, we are here—at least from the look of Fig. 5.3a—rather *adding* something, since a region of the Schwarzschild spacetime appears twice in the final construction. Let us see what happens if we do something similar with the Euclidean cone. We return to Fig. 5.1, but instead of cutting away a wedge—which will be referred to as a "conical deficit"—we tear the plane apart with the effect that an identical wedge is being added. We will refer to this case as a "conical excess". This procedure is difficult to accomplish with a piece of paper, and the result will not really fit into Euclidean space. But we can visualize it by embedding it as a spacelike surface in $(2+1)$-dimensional Minkowski space, where it will look like the ordinary cone of Fig. 5.4. Note that an increase in the conical excess would steepen the slope of the cone. In the limit, when the excess angle approaches infinity, we can therefore see the result as a light cone in Minkowski space. Anyhow, with the same procedure we used to regularize the ordinary

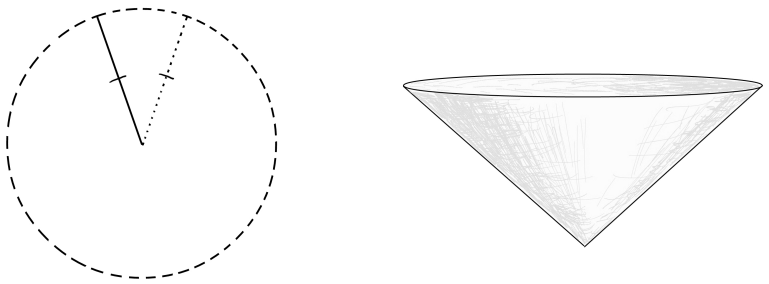

(a) Adding a wedge to the plane produces a cone...

(b) ...which can be embedded in flat spacetime.

Figure 5.4: Another cone.

[1]By "smooth" we here mean that the metric is C^1.

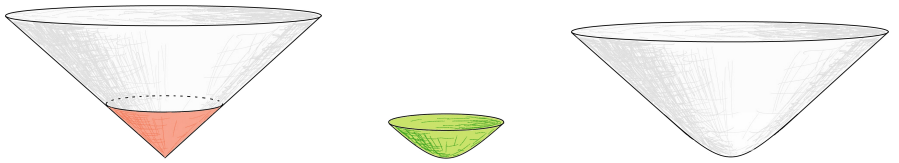

Figure 5.5: Replacing the tip of a cone with a piece of a hyperbolic plane.

cone, we can regularize this one by cutting and gluing. Replacing the tip with a piece of a sphere will not work, however, but a piece of a hyperbolic plane will fit, as shown in Fig. 5.5. The striking difference between the cases of conical deficit and excess is thus that the former can be made smooth by adding a piece of *positive* curvature (e.g. a sphere), while the latter can only be made smooth by adding *negative* curvature (e.g. a hyperbolic plane).

So, again, what are the consequences of tearing apart the Schwarzschild spacetime as in Haggard's and Rovelli's model? Does the tearing result in a region with negative curvature, corresponding to negative energy density? In order to answer that question, more information than what is given about the spacelike hypersurfaces bounding the quantum region is needed. Exactly what has to be taken into account will be made clear in the following sections, where the two cases of conical deficit and excess will be dealt with in turn.

Conical deficit

Take a look at Fig. 5.6a. The figure shows $(1+1)$-dimensional Minkowski space, where a wedge (grey) has been cut out along two spacelike straight lines meeting at the origin of the coordinate system we will later use. As the edges are identified, the result is some sort of cone, which could be embedded as a timelike surface in $(2+1)$-dimensional Minkowski space. Now, we make another cut, along two spacelike geodesics intersecting twice due to the identification, removing the red segment containing the singularity. As before the idea is to fill the hole thus created with a piece of a curved spacetime, making our cone smooth. If we stick to spacetimes of constant curvature, we have two choices: de Sitter space which has positive curvature, and anti-de Sitter space which has negative curvature. Which one should we choose?

The answer can be found in the Lorentzian version of the Gauss-Bonnet theorem (see e.g. Law, 1992), which reads

$$\int_S K \,\mathrm{d}S + \int_\gamma k_g \,\mathrm{d}s + \sum \theta_{\mathrm{ext}} = 2\pi i \chi(S) \,, \tag{5.1}$$

where K is the Gaussian curvature of a two-surface S, and k_g and θ_{ext} the

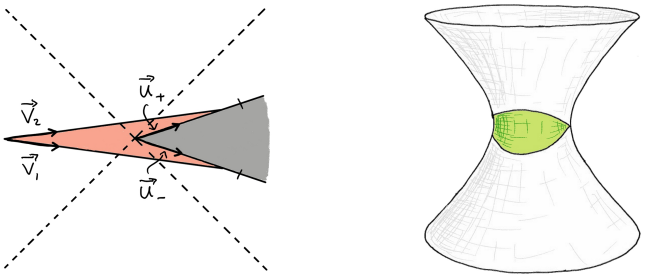

(a) Minkowski space. **(b)** de Sitter space.

Figure 5.6: The tip of a cone (red) can be replaced by a patch of a spacetime with positive curvature (green).

geodetic curvature and exterior angles of its boundary γ. We will only consider cases where the Euler characteristic χ is one. There are a few difficulties involved here, however. If we were to draw a circle around the origin in Minkowski space, its curvature would diverge at those four points where the tangent vector changes its causal character. Therefore, we insist that smooth segments of the boundary are everywhere spacelike or timelike. This explains the choice of boundary of the hole that was cut out in Fig. 5.6a. But as a result, this boundary has corners, and it is not very clear how to define the "exterior angle" of such corners. There is no continuous isometry taking the vector $-\vec{v}_2$ in Fig. 5.6a to the vector $\vec{v}_1$, for instance. For now, let us just state that this is where the mysterious imaginary term on the right hand side of the Gauss-Bonnet theorem (5.1) comes in.

Given the boundary of the hole that we cut out, we will now, with help from the Gauss-Bonnet theorem, be able to determine the sign of the Gaussian curvature K of the patch filling the hole. Let us do this as an explicit exercise. Let t and x be coordinates in Minkowski space with line element

$$\mathrm{d}s^2 = -\mathrm{d}t^2 + \mathrm{d}x^2 \,. \tag{5.2}$$

Choose the straight lines

$$t = \pm x \tanh\frac{\mu}{2} \tag{5.3}$$

at positive x to be identified. Their respective unit tangent vectors $\vec{u}_\pm$ are

$$u^a_\pm = \pm\sinh\frac{\mu}{2}\,\partial^a_t + \cosh\frac{\mu}{2}\,\partial^a_x \,. \tag{5.4}$$

The line at negative t is mapped to that at positive t under a boost by a hyperbolic angle μ which is taken to be positive. As these two lines are identified, so are their tangent vectors $\vec{u}_+$ and $\vec{u}_-$. The tip of the cone resulting from this

identification is now removed by cutting away a segment chosen to be bounded by two straight lines with tangent vectors

$$\begin{aligned} v_1^a &= -\sinh\frac{\mu}{4}\,\partial_t^a + \cosh\frac{\mu}{4}\,\partial_x^a\,, \\ v_2^a &= \sinh\frac{\mu}{4}\,\partial_t^a + \cosh\frac{\mu}{4}\,\partial_x^a\,. \end{aligned} \tag{5.5}$$

The position of these lines will be as indicated in Fig. 5.6a. For definiteness, we fix the length of each of the lines, between the two points of intersection, to be L. Since the hole is thus bounded by geodesics, the second term on the left hand side of the Gauss-Bonnet theorem (5.1) vanishes. Instead we will have to worry about exterior angles, and how they are defined in a Lorentzian context. The rules of the game are given for the current example.

There are two corners of the boundary; let us concentrate on the exterior angle at the right corner in Fig. 5.6a, as the boundary is traversed counter clockwise. Start along the line with tangent $\vec{v}_1$ moving to the right. As the point of intersection is reached, the tangent switches direction to $-\vec{v}_2$ according to the chosen orientation. First, $\vec{v}_1$ is taken to the tangent $\vec{u}_-$ of one of the identification lines by boosting it by an amount $-\mu/4$. The vector $\vec{u}_-$ is then identified with the tangent $\vec{u}_+$ of the other identification line, which can by taken to the vector $\vec{v}_2$ by a boost of $-\mu/4$. So, the total hyperbolic angle between $\vec{v}_1$ and $\vec{v}_2$ is $-\mu/2$. Finally, when reflecting the vector $\vec{v}_2$ to $-\vec{v}_2$ a term $i\pi$ is added. Thus, the exterior angle of the right corner is

$$\theta_{\text{ext}} = -\frac{\mu}{2} + i\pi\,. \tag{5.6}$$

The exterior angle of the left corner is the same. Inserting this result into Eq. (5.1) we find that

$$KA = \mu \tag{5.7}$$

for a patch with constant Gaussian curvature K and area A, that we wish to use for filling the hole. According to the Gauss-Bonnet theorem, we see that this patch must have positive curvature.

$(1+1)$-dimensional de Sitter space, defined as the hyperboloid

$$X^2 + Y^2 - T^2 = \ell^2\,, \tag{5.8}$$

embedded in $(2+1)$-dimensional Minkowski space with metric

$$\mathrm{d}s^2 = -\mathrm{d}T^2 + \mathrm{d}X^2 + \mathrm{d}Y^2\,, \tag{5.9}$$

is therefore perfect for our needs. There, we can find spacelike geodesics intersecting twice, for instance the curves given as the intersection of the planes

$$T = \pm X \tanh\frac{\mu}{4} \tag{5.10}$$

in the embedding spacetime, with the surface (5.8) of de Sitter space. These are chosen so as to have the same hyperbolic angle between them as the curves bounding the hole of the cone. We now choose the scale ℓ of de Sitter space as

$$\ell = \frac{L}{\pi} \,, \tag{5.11}$$

thus making sure that the length of these two geodesics between the points where they intersect is L. With these choices the patch of de Sitter space bounded by the two geodesics—shown as the green patch in Fig. 5.6b—fits perfectly into the red hole of the cone in Fig. 5.6a.

Just as a double check we may verify that the form (5.7) of the Gauss-Bonnet theorem for this patch holds. The Gaussian curvature of de Sitter space is

$$K = \frac{1}{\ell^2} \,, \tag{5.12}$$

and the area of the patch considered is found to be

$$A = \mu \ell^2 \,. \tag{5.13}$$

We immediately see that all the pieces of the puzzle fit together.

The conclusion, however, is not that a conical deficit inevitably leads to positive curvature. If the wedge that is cut out of spacetime is bounded by *timelike* geodesics, a treatment analogous to the above shows that the tip of the cone must be replaced by a patch with *negative* curvature.

Conical excess

The question now is what happens in the case of conical excess. The quick answer to that question is given by Fig. 5.7. Here, two spacelike lines—marked in Fig. 5.7a—are identified as Minkowski space is torn apart, and a wedge identical to the region bounded by these two lines is added. Let us cut out a diamond (red) surrounding the conical singularity along four geodesics. In order to see that the figure actually shows a diamond, you will have to imagine that you grab the two spikes to the right, and then pull them towards each other, past each other, until the lines with marks touch. Summing the exterior angles of the boundary of the diamond, the Gauss-Bonnet theorem will tell us that the spacetime we wish to attach to it must have negative curvature. Indeed, a piece of $(1+1)$-dimensional anti-de Sitter space bounded by four spacelike geodesics—as shown in green in Fig. 5.7b—fits perfectly into the hole that is cut out of the cone. And again, if the conical excess is created by an identification of two timelike rather than spacelike lines, the result will be the opposite: the conical singularity can be replaced only by a piece of a spacetime with positive curvature.

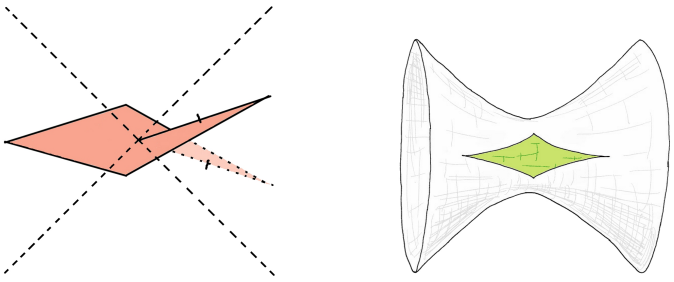

(a) Minkowski space. **(b)** Anti-de Sitter space.

Figure 5.7: The tip of a cone (red) can be replaced by a patch of a spacetime with negative curvature (green).

If we want to apply these results to the model by Haggard and Rovelli, it would seem like the cone depicted in Fig. 5.7 is the relevant case to consider. But their proposal is not detailed enough to draw any definite conclusions. However, it has given an opportunity to study Lorentzian cones. At least, these cones tell us that we need to take care when exploiting the technique of cutting and gluing for creating spacetime models. If we want the model to be physically realistic, avoiding negative curvatures, the cones provide a key to the allowed procedures. But they are also interesting in their own right. The fun exercise in cutting and gluing that they provide illustrates an interesting difference between Euclidean space and Minkowski space.

With these remarks, this thesis ends.

Sammanfattning

Idén om svarta hål uppstod som en teoretisk förutsägelse utifrån den allmänna relativitetsteorin. Numera är deras faktiska existens föga ifrågasatt; astronomiska observationer tyder på att svarta hål ofta utgör navet kring vilket stjärnor rör sig i galaxer. Så anses till exempel vara fallet i vår egen galax Vintergatan. Trots att teorin för svarta hål har varit med oss i decennier, så finns det fortfarande intressanta frågor att besvara. Den här doktorsavhandlingen och de fyra medföljande artiklarna berör några av dessa frågor.

En utmanande teoretisk aspekt av svarta hål ligger i själva definitionen av dem. Ett svart hål definieras av dess händelsehorisont. Händelsehorisonten utgör en gräns i rumtiden sådan att den som väl passerat den – och därmed färdats in i det svarta hålet – aldrig någonsin kan ta sig ut igen. Detsamma gäller ljusstrålar; på så sätt kan en observatör utanför det svarta hålet aldrig se vad som händer i dess inre. Problemet med händelsehorisonten är att den inte kan observeras genom en lokal mätning. Det ter sig således som om vi aldrig skulle kunna avgöra ifall vi i just detta ögonblick passerar gränsen för ett mycket stort svart hål. I princip skulle det dock kunna finnas tecken på att så har skett. Ett sådant tecken skulle vara närvaron av en så kallad *fångad yta*. En sådan yta är något så ointuitivt som en sluten yta sådan att ljusstrålar som skickas ut vinkelrätt från den, snarare än att avlägsna sig från varandra, istället närmar sig varandra. Detta kan förstås om en föreställer sig att rummet i sig krymper med en sådan fart att inte ens ljuset hänger med. En sådan bild av händelseförloppet gör det troligt att fångade ytor bara kan existera i närvaro av mycket stark gravitation, såsom inuti ett svart hål. I den första av de medföljande artiklarna studeras just fångade ytor i en enkel modell som beskriver en kropp som kollapsar och ger upphov till ett svart hål.

Den andra artikeln är av något mer matematisk karaktär. Handlingen här utspelar sig kring ett svart hål som har elektrisk laddning. Enligt teorin finns det en övre gräns för hur stor denna laddning kan vara, och i det fall den är maximal sägs det svarta hålet vara extremt. Det extrema svarta hålets egenskaper skiljer sig i många delar från det icke-extrema. Rent matematiskt tycks dock gränsdragningen då laddningen närmar sig sitt maximala värde vara tvetydig; i själva verket kan resultatet vara en helt annan rumtid, som inte över

huvud taget beskriver ett svart hål. Vilka val som måste göras för att definiera en tydlig gräns reddes ut av Geroch redan 1969. Hans ursprungsartikel är dock i vissa delar något svårläst, och målet med vår artikel är att ge en pedagogisk illustration av hans definition. Här förklaras gränsdragningsproceduren i form av bilder, så att vi med egna ögon kan se vad som händer matematiskt då laddningen hos det svarta hålet ökar.

Nästa fråga som avhandlas är den om hur stor volymen hos ett svart hål är. Det är en fråga som inte är tydligt definierad inom teorin; svaret är relativt. I en artikel av Christodoulou & Rovelli (2015), ges istället svaret på hur stor den *maximala* volymen är hos ett svart hål som bildats genom att en sfäriskt symmetrisk kropp kollapsat. De finner att det svarta hålet i Vintergatans mitt – som gott och väl skulle få plats innanför Merkurius bana – skulle kunna rymma en miljon solsystem! De betraktar dock inte roterande svarta hål, och med tanke på att de svarta hål som existerar ute i rymden roterar, kan en fråga sig om dessa är lika rymliga. Det är de, vilket visas i den tredje artikeln.

Den sista medföljande artikeln handlar om den berömda Penroseolikheten. Idén bakom dess uppkomst involverar gravitationskollaps, fångade ytor, svarta hål och hypotesen om kosmisk censur. Den kan dock formuleras om till ett rent geometriskt samband i en platt rumtid i frånvaro av gravitation. Det har visat sig att olikheten håller i många fall, men det stora målet är att visa att den gäller i allmänhet. I vår artikel presenteras en leksaksmodell av problemet. Förenklingen ligger i att betrakta en rumtid som – utöver en tidsdimension – endast har *två* rumsliga dimensioner. Genom att härma egenskaper hos originalolikheten kan en geometrisk olikhet formuleras och även bevisas i denna tredimensionella rumtid. Denna nya olikhet är i sig intressant, men dessutom skulle dess bevis i bästa fall kunna ge nya idéer till framgångsgrika strategier för att nå det stora målet.

Slutligen innehåller avhandlingen ett avsnitt om koner i rumtiden. En enkel kon med valfri spetsighet kan lätt skapas hemma med hjälp av en bit papper, en sax och lite tejp. Men risken med dylika klipp-och-klistrametoder i *rumtiden* är att modellen som därmed skapas blir ofysikalisk. Här utreds vilka tillvägagångssätt som är fysikaliskt acceptabla vid ett sådant ingrepp.

Sammantaget utgör dessa olika bidrag en samling intressanta aspekter av svarta hål och deras geometri.

References

ANDERSSON L., MARS M., AND SIMON W. 2008 "Stability of Marginally Outer Trapped Surfaces and Existence of Marginally Outer Trapped Tubes" *Adv. Theor. Math. Phys.* **12** 853

ASHTEKAR A. AND KRISHNAN B. 2004 "Isolated and Dynamical Horizons and Their Applications" *Living Rev. Rel.* **7** 10

BAÑADOS M., HENNEAUX M., TEITELBOIM C., AND ZANELLI J. 1993 "Geometry of the 2+1 Black Hole" *Phys. Rev. D* **48** 1506

BAÑADOS M., TEITELBOIM C., AND ZANELLI J. 1992 "Black Hole in Three-Dimensional Spacetime" *Phys. Rev. Lett.* **69** 1849

BARCELÓ C., CARBALLO-RUBIO R., AND GARAY L. J. 2014 "Mutiny at the White-Hole District" *Int. J. Mod. Phys. D* **23** 1442022

BEN-DOV I. 2007 "Outer Trapped Surfaces in Vaidya Spacetimes" *Phys. Rev. D* **75** 064007

BENGTSSON I. AND SENOVILLA J. M. M. 2009 "Note on Trapped Surfaces in the Vaidya Solution" *Phys. Rev. D* **79** 024027

BENGTSSON I. AND SENOVILLA J. M. M. 2011 "Region with Trapped Surfaces in Spherical Symmetry, Its Core, and Their Boundaries" *Phys. Rev. D* **83** 044012

BERGQVIST G. 1997 "On the Penrose Inequality and the Role of Auxiliary Spinor Fields" *Class. Quantum Grav.* **14** 2577

BOOTH I. 2005 "Black Hole Boundaries" *Can. J. Phys.* **83** 1073

BRAY H. L. 2001 "Proof of the Riemannian Penrose Inequality Using the Positive Mass Theorem" *J. Diff. Geom.* **59** 177

BRENDLE S. AND WANG M. T. 2014 "A Gibbons-Penrose Inequality for Surfaces in Schwarzschild Spacetime" *Commun. Math. Phys.* **330** 33

CARTER B. 1966 "Complete Analytic Extension of the Symmetry Axis of Kerr's Solution of Einstein's Equations" *Phys. Rev.* **141** 1242

CHRISTODOULOU D. 1984 "Violation of Cosmic Censorship in the Gravitational Collapse of a Dust Cloud" *Commun. Math. Phys.* **93** 171

CHRISTODOULOU D. 1999 "The Instability of Naked Singularities in the Gravitational Collapse of a Scalar Field" *Ann. Math.* **149** 183

CHRISTODOULOU M. AND DE LORENZO T. 2016 "Volume Inside Old Black Holes" *Phys. Rev. D* **94** 104002

CHRISTODOULOU M. AND ROVELLI C. 2015 "How Big is a Black Hole?" *Phys. Rev. D* **91** 064046

DAFERMOS M. 2005 "The Interior of Charged Black Holes and the Problem of Uniqueness in General Relativity" *Commun. Pure Appl. Math.* **58** 445

DI CARLO V. 2007 *Conformal Compactification and Anti-de Sitter Space*, Master's Thesis, KTH Royal Institute of Technology

EARDLEY D. M. 1998 "Black Hole Boundary Conditions and Coordinate Conditions" *Phys. Rev.D̃* **57** 2299

EINSTEIN A. 1915 "Der Feldgleichungen der Gravitation" *Preuss. Akad. Wiss. Berlin, Sitzber.* 844

EINSTEIN A. 1941 "Demonstration of the Non-Existence of Gravitational Fields with a Non-Vanishing Total Mass Free of Singularities" *Univ. Nac. Tucumán Rev. A* **2** 5

FINKELSTEIN D. 1958 "Past-Future Asymmetry of the Gravitational Field of a Point Particle" *Phys. Rev.* **110** 965

FRIEDMANN A. 1922 "Über die Krümmung des Raubes" *Z. Phys.* **10** 377

FRONSDAL C. 1959 "Completion and Embedding of the Schwarzschild Solution" *Phys. Rev.* **116** 778

FULLER R. W. AND WHEELER J. A. 1962 "Causality and Multiply Connected Space-Time" *Phys. Rev.* **128** 919

GEROCH R. 1969 "Limits of Spacetimes" *Commun. Math. Phys.* **13** 180

GEROCH R. 1973 "Energy Extraction" *Ann. N. Y. Acad. Sci.* **224** 108

GIBBONS G. W. 1973 *Some Aspects of Gravitational Radiation and Gravitational Collapse*, Ph.D. Thesis, Cambridge University

GIBBONS G. W. 1984 "The Isoperimetric and Bogomolny Inequalities for Black Holes", in *Global Riemannian Geometry*, ed. T. J. WILLMORE AND N. J. HITCHIN, Ellis Horwood

GRAVES J. C. AND BRILL D. R. 1960 "Oscillatory Character of Reissner-Nordström Metric for an Ideal Charged Wormhole" *Phys. Rev.* **120** 1507

HAGGARD H. M. AND ROVELLI C. 2015 "Black Hole Fireworks: Quantum-Gravity Effects Outside the Horizon Spark Black to White Hole Tunneling" *Phys. Rev. D* **92** 104020

HAWKING S. W. AND ELLIS G. F. R. 1973 *The Large Scale Structure of Space-Time*, Cambridge University Press, Cambridge

HAYWARD S. A. ed. 2013 *Black Holes: New Horizons*, World Scientific, Singapore

HOLST S. 2000 *Horizons and Time Machines – Global Structures in Locally Trivial Spacetimes*, Ph.D. Thesis, Stockholm University

HUISKEN G. AND ILMANEN T. 2001 "The Inverse Mean Curvature Flow and the Riemannian Penrose Inequality" *J. Diff. Geom.* **59** 353

JAKOBSSON E. 2011 *Trapped Surfaces in 2+1 Dimensions*, Master's Thesis, Stockholm University

JAKOBSSON E. 2014 *Black Holes and Trapped Surfaces*, Licentiate Thesis, Stockholm University

JANG P. S. AND WALD R. M. 1977 "The Positive Energy Conjecture and the Cosmic Censorship" *J. Math. Phys.* **18** 41

JEBSEN J. T. 1921 "Über die allgemeinen kugelsymmetrischen Lösungen der Einsteinschen Gravitationsgleichungen im Vakuum" *Ark. Mat. Astr. Fys.* **15**

KERR R. P. 1963 “Gravitational Field of a Spinning Mass as an Example of Algebraically Special Metrics” *Phys. Rev. Lett.* **11** 237

KRUSKAL M. D. 1960 “Maximal Extension of Schwarzschild Metric” *Phys. Rev.* **119** 1743

LAW P. R. 1992 “Neutral Geometry and the Gauss-Bonnet Theorem for Two-Dimensional Pseudo-Riemannian Manifolds” *Rocky Mountain J. Math.* **22** 1365

MARS M. AND SORIA A. 2012 “On the Penrose Inequality for Dust Null Shells in the Minkowski Spacetime of Arbitrary Dimension” *Class. Quantum Grav.* **29** 135005

MARS M. AND SORIA A. 2014 “Geometry of Normal Graphs in Euclidean Space and Applications to the Penrose Inequality in Minkowski” *Ann. Henri Poincaré* **15** 1903

MARS M. AND SORIA A. 2016 “On the Penrose Inequality Along Null Hypersurfaces” *Class. Quantum Grav.* **33** 115019

NORDSTRÖM G. 1918 “On the Energy of the Gravitational Field in Einstein’s Theory” *Proc. Kon. Ned. Akad. Wet.* **20** 1238

O’NEILL B. 1995 *The Geometry of Kerr Black Holes*, A K Peters, Wellesley, Massachusetts

ONG Y. C. 2015 “The Persistence of the Large Volumes in Black Holes” *Gen. Relativ. Gravit.* **47** 88

OPPENHEIMER J. R. AND SNYDER H. 1939 “On Continued Gravitational Contraction” *Phys. Rev.* **56** 455

PENROSE R. 1965 “Gravitational Collapse and Space-Time Singularities” *Phys. Rev. Lett.* **14** 57

PENROSE R. 1968 “Structure of Space-Time” in *Battelle Rencontres: 1967 lectures in mathematics and physics*, ed. C. M. DEWITT AND J. A. WHEELER, W. A. Benjamin, New York

PENROSE R. 1969 “Gravitational Collapse: The Role of General Relativity” *Riv. Nuovo Cimento* **1** 252

PENROSE R. 1973 “Naked Singularities” *Ann. N. Y. Acad. Sci.* **224** 125

POISSON E. 2004 *A Relativist’s Toolkit: The Mathematics of Black Hole Mechanics*, Cambridge University Press, Cambridge

POISSON E. AND ISRAEL W. 1990 “Internal Structure of Black Holes” *Phys. Rev. D* **41** 1796

REISSNER H. 1916 “Über die Eigengravitation des elektrischen Felds nach der Einsteinschen Theorie” *Ann. Physik* **50** 106

ROESCH H. 2016 “Proof of a Null Penrose Conjecture Using a New Quasi-Local Mass” arXiv:1609.02875 [gr-qc]

SAUTER J. 2008 *Foliations of Null Hypersurfaces and the Penrose Inequality*, Ph.D. Thesis, ETH Zürich

SCHOEN R. AND YAU S.-T. 1979 “On the Proof of the Positive Mass Conjecture in General Relativity” *Commun. Math. Phys.* **65** 45

SCHOEN R. AND YAU S.-T. 1981 “Proof of the Positive Mass Theorem II” *Commun. Math. Phys.* **79** 231

SCHWARZSCHILD K. 1916 “Über das Gravitationsfeld eines Massenpunktes nach der Einsteinschen Theorie” *Sitzber. Preuss. Akad. Wiss. Physik.-Math. Kl.* 189

SENOVILLA J. M. M. 2007 “Classification of Spacelike Surfaces in Spacetime” *Class. Quantum Grav.* **24** 3091

SENOVILLA J. M. M. AND GARFINKLE D. 2015 “The 1965 Penrose Singularity Theorem” *Class. Quantum Grav.* **32** 124008

SIMPSON M. AND PENROSE R. 1973 "Internal Instability in a Reissner-Nordström Black Hole" *Int. J. Theor. Phys.* **7** 183

THORNBURG J. 2007 "Event and Apparent Horizon Finders for 3+1 Numerical Relativity" *Living Rev. Rel.* **10** 3

TOD K. P. 1985 "Penrose's Quasi-Local Mass and the Isoperimetric Inequality for Static Black Holes" *Class. Quantum Grav.* **2** L65

VAIDYA P. C. 1951 "The Gravitational Field of a Radiating Star" *Proc. Indian Acad. Sci. A* **33** 264

VAIDYA P. C. 1953 "Newtonian Time in General Relativity" *Nature* **171** 260

WALD R. M. AND IYER V. 1991 "Trapped Surfaces in the Schwarzschild Geometry and Cosmic Censorship" *Phys. Rev. D* **44** R3719

WITTEN E. 1981 "A New Proof of the Positive Energy Theorem" *Commun. Math. Phys.* **80** 381